Mon. Not. R. Astron. Soc. **000**, 1–18 (2011) Printed 27 June 2011 (MN LATEX style file v2.2)

Blazhko RR Lyrae light curves as modulated signals

J. M. Benkő⋆, R. Szabó, and M. Paparó
Konkoly Observatory, Konkoly Thege M. u. 15-17., H-1121 Budapest, Hungary

Accepted 2011 June 23. Received 2011 June 23; in original form 2011 April 28

ABSTRACT
We present an analytical formalism for the description of Blazhko RR Lyrae light curves in which employ a treatment for the amplitude and frequency modulations in a manner similar to the theory of electronic signal transmitting. We assume monoperiodic RR Lyrae light curves as carrier waves and modulate their amplitude (AM), frequency (FM), phase (PM), and as a general case we discuss simultaneous AM and FM. The main advantages of this handling are the following: (i) The mathematical formalism naturally explains numerous light curve characteristics found in Blazhko RR Lyrae stars such as mean brightness variations, complicated envelope curves, non-sinusoidal frequency variations. (ii) Our description also explains properties of the Fourier spectra such as apparent higher-order multiplets, amplitude distribution of the side peaks, the appearance of the modulation frequency itself and its harmonics. In addition, comparing to the traditional method, our light curve solutions reduce the number of necessary parameters. This formalism can be applied to any type of modulated light curves, not just for Blazhko RR Lyrae stars.

Key words: methods: analytical — methods: data analysis — stars: oscillations — stars: variables: general — stars: variables: RR Lyrae

1 INTRODUCTION

The Blazhko effect (Blazhko 1907) is a periodic amplitude and phase variation of the RR Lyrae variable stars' light curve. The typical cycle lengths of these variations are about of 10-100 times longer than the main pulsation periods (0.3−0.7 d). Almost half of the RR Lyrae stars pulsating in their fundamental mode (type RRab) and a smaller but non-negligible fraction of the first overtone mode pulsating stars (type RRc) show the effect (Jurcsik et al. 2009c; Chadid et al. 2009; Kolenberg et al. 2010; Benkő et al. 2010). It is usually interpreted as a modulation or a beating phenomenon, but both hypotheses have their own problems. The beating picture describes the main feature of the light curves and Fourier spectra well (see Breger & Kolenberg 2006; Kolenberg et al. 2006), but reproducing phase variations, multiplet structures found in certain stars' Fourier spectra (Jurcsik et al. 2008; Chadid et al. 2010) in this framework is not possible. On the other side, the stars showing doublet structures in their Fourier spectra (Alcock et al. 2000, 2003; Moskalik & Poretti 2003) seemed to be contradicted with the modulation picture.

In this paper we describe the Blazhko effect as a modulation, and derive the mathematical consequences of this assumption by developing a consistent analytical framework. Using this framework we demonstrate that many light curve characteristics are naturally identified as mathematical consequences of the modulation assumption. By disentangling these features we get closer to the physics behind the Blazhko effect.

⋆ E-mail: benko@konkoly.hu

The possibility of the modulation/Blazhko effect have been raised for many types of pulsating stars from Cepheids to δ Scuti stars (see e.g. Koen 2001; Henry, Fekel & Henry 2005; Moskalik & Kołaczkowski 2009; Breger 2010; Poretti et al. 2011). The main motivation of this paper is the mathematical description of the Blazhko RR Lyrae stars' light curves and investigate their properties. Most of our results can be applied directly to any other types of variable stars, where modulation is suspected. Our deduced formulae and the related phenomena may help to prove or reject the modulation hypothesis.

The basic idea of this paper was raised in Benkő et al. (2009). Modulation is a technique that has been used in electronic communication for a long time, mostly for transmitting information signal via a radio carrier wave. In those cases, the carrier wave is a sinusoidal electromagnetic (radio) wave that is modulated by a (generally non-periodic) information signal (e.g. speech, music). In this paper the formalism developed by engineers for broadcasting radio signals has been modified such a way that we assumed a monoperiodic non-modulated RR Lyrae light variation as a carrier wave. While for communication usually only one type of modulation is applied we allow both types of modulations (amplitude and angle).

In Section 2 we present a collection of classical formulae that are well-known in physics of telecommunications (Carson 1922; van der Pol 1930; Roder 1931). Some of the more complicated cases (multiple modulations, recursive or cascade modulations) were investigated by mathematicians who developed the theory of electric sound synthesizers in the years of 1960s and '70s. The formulae are modified to describe the modulated light curves in Sec. 3 and investigated by a step-by-step process from the simplest

cases to the more complex ones. Section 4 compares the numerical behaviour of the traditional method and this one. Section 5 summarizes our results.

2 BASIC FORMULAE

In this section we briefly review some classical definitions and formulae (see e.g. Newkirk & Karlquist 2004; Schottstaedt 2003) that will be used through the next sections. The simplest periodic signal is a sinusoidal function. It has three basic parameters: amplitude, frequency and phase and any of these can be modulated.

2.1 Amplitude modulation

The amplitude modulation (AM) is the simplest of the three cases. Let the carrier wave $c(t)$ be a simple sinusoidal signal as

$$c(t) = U_{\rm c}\sin(2\pi f_{\rm c}t + \varphi_{\rm c}), \tag{1}$$

where $U_{\rm c}$, $f_{\rm c}$ and $\varphi_{\rm c}$ constant parameters are the amplitude, frequency and initial phase of the carrier wave, respectively.

Let $U_{\rm m}(t)$ represent an arbitrary waveform that is the message to be transmitted. The transmitter uses the information signal $U_{\rm m}(t)$ to vary the amplitude of the carrier $U_{\rm c}$ to produce a modulated signal:

$$U_{\rm AM}(t) = [U_{\rm c} + U_{\rm m}(t)]\sin(2\pi f_{\rm c}t + \varphi_{\rm c}). \tag{2}$$

In the simplest case, where the modulation is also sinusoidal

$$U_{\rm m}(t) = U_{\rm m}^{\rm A}\sin(2\pi f_{\rm m}t + \varphi_{\rm m}^{\rm A}). \tag{3}$$

Substituting Eq. (3) into (2) and using basic trigonometrical identities, expression (2) can be rewritten as

$$U_{\rm AM}(t) = U_{\rm c}\sin(2\pi f_{\rm c}t + \varphi_{\rm c}) + \frac{U_{\rm m}^{\rm A}}{2}\left\{\sin\left[2\pi\left(f_{\rm c} - f_{\rm m}\right)t + \varphi^{-}\right] + \sin\left[2\pi\left(f_{\rm c} + f_{\rm m}\right)t + \varphi^{+}\right]\right\}, \tag{4}$$

where $\varphi^{-} = \varphi_{\rm c} - \varphi_{\rm m}^{\rm A} + \pi/2$ and $\varphi^{+} = \varphi_{\rm c} + \varphi_{\rm m}^{\rm A} - \pi/2$. The initial shifts ($\pm\pi/2$) appear because we used (through all this paper) a sinusoidal representation instead of sin and cos functions.

The exact analytical Fourier transformation of (4) is given in Appendix A, however, the basic structure of the frequency spectrum can be easily read off from Eq. (4). Since the Fourier spectrum of a single sinusoidal function shows a peak at the frequency of the sinusoid, from the above expression (4) the well-known triplet structure composed of the peaks $f_{\rm c}$ and $f_{\rm c} \pm f_{\rm m}$ can be seen. The amplitude of the side-peaks $f_{\rm c} \pm f_{\rm m}$ are always equal. The Fourier amplitude of the carrier wave ($\pi\sqrt{2\pi}U_{\rm c}$), that represents the energy at the carrier frequency, is constant.

The ratio of the carrier wave amplitude $A(f_{\rm c})$ and the side peaks $A(f_{\rm c} \pm f_{\rm m})$ are connected to the modulation depth. We rewrite Eq. (2) as

$$U_{\rm AM}(t) = \left[1 + \frac{U_{\rm m}(t)}{U_{\rm c}}\right]c(t). \tag{5}$$

If $U_{\rm m}(t)$ is a bounded function, let $U_{\rm m}^{\max}$ represent the maximum value of this modulation function, then *modulation depth* is defined as $h = U_{\rm m}^{\max}/U_{\rm c}$. In the above discussed sinusoidal case $h = U_{\rm m}^{\rm A}/U_{\rm c}$ and $A(f_{\rm c} \pm f_{\rm m})/A(f_{\rm c}) = \frac{1}{2}h$. In other words, the amplitude of the central peak is twice of the side peak highs.

2.2 Angle modulations

The phase and frequency modulations together are called angle modulations. Since, when we assume the sinusoidal carrier wave Eq. (1) as $c(t) = U_{\rm c}\sin[\Theta(t)]$, the $\Theta(t) = 2\pi f_{\rm c}t + \varphi_{\rm c}$ denotes the angle part of the function.

Phase modulation (PM) changes the phase angle of the carrier signal. Suppose that the modulating or message signal is $U_{\rm m}(t)$, then $\Theta(t) = 2\pi f_{\rm c}t + [\varphi_{\rm c} + U_{\rm m}(t)]$. Let $U_{\rm m}(t)$ be again a bounded function. In this case we can define a constant as: $k_{\rm PM} = |U_{\rm m}^{\max}(t)|/2$. This transforms the modulated signal

$$U_{\rm PM}(t) = U_{\rm c}\sin\left[2\pi f_{\rm c}t + k_{\rm PM}U_{\rm m}^{\rm P}(t) + \varphi_{\rm c}\right], \tag{6}$$

where $|U_{\rm m}^{\rm P}(t)| \leqslant 1$. The *instantaneous frequency* of the modulated signal is

$$f(t) = \frac{{\rm d}\Theta}{{\rm d}t} = f_{\rm c} + k_{\rm PM}\frac{{\rm d}U_{\rm m}^{\rm P}(t)}{{\rm d}t}. \tag{7}$$

Frequency modulation (FM) uses the modulation signal $U_{\rm m}(t)$ to vary the carrier frequency. $\Theta(t) = 2\pi f(t)t + \varphi_{\rm c}$ and here the instantaneous frequency $f(t)$ is modulated by the signal of $k_{\rm FM}U_{\rm m}^{\rm F}(t)$ as

$$f(t) = f_{\rm c} + k_{\rm FM}U_{\rm m}^{\rm F}(t). \tag{8}$$

In this equation $k_{\rm FM}$ is the frequency deviation, which represents the maximum shift from $f_{\rm c}$ in one direction, assuming $U_{\rm m}^{\rm F}(t)$ is limited to the range $(-1, \ldots, +1)$. Using the definitions of the instantaneous frequency and phase, expression (8) can be rewritten as $\Theta(t) = 2\pi f_{\rm c}t + 2\pi k_{\rm FM}\int_0^t U_{\rm m}^{\rm F}(\tau)d\tau + \varphi_{\rm c}$. The modulated signal is

$$U_{\rm FM}(t) = U_{\rm c}\sin\left[2\pi f_{\rm c}t + 2\pi k_{\rm FM}\int_0^t U_{\rm m}^{\rm F}(\tau)\,d\tau + \varphi_{\rm c}\right]. \tag{9}$$

This definition of FM is the least intuitive of the three Eqs (2, 6 and 9). If we compare Eqs (6) and (9) we realize that the modulation signals are in derivative-integral connection with each other. In practice, we have modulating signals that can be represented by analytical functions. Therefore, when we detect an FM or PM signal without any previous knowledge about them, it is impossible to distinguish between FM and PM signals.

First, let the modulating signal be represented by a sinusoidal wave with a frequency $f_{\rm m}$. The integral of such a signal is

$$U_{\rm m}^{\rm F}(t) = \frac{U_{\rm m}^{\rm F}}{2\pi f_{\rm m}}\sin\left(2\pi f_{\rm m}t + \varphi_{\rm m}^{\rm F}\right). \tag{10}$$

Thus, in this case Eq. (9) gives

$$U_{\rm FM}(t) = U_{\rm c}\sin\left[2\pi f_{\rm c}t + \eta\sin\left(2\pi f_{\rm m}t + \varphi_{\rm m}^{\rm F}\right) + \varphi_{\rm c}\right], \tag{11}$$

where the *modulation index* is defined as $\eta = (k_{\rm FM}U_{\rm m}^{\rm F})/f_{\rm m}$. Eq. (11) can be deduced from Eq. (6) as well. The only difference is the value of $\eta = k_{\rm PM}U_{\rm m}^{\rm P}$, which is independent of the modulation frequency $f_{\rm m}$. Let us transcribe Eq. (11) using relations for trigonometrical and Bessel functions (Abramowitz & Stegun 1972) as:

$$U_{\rm FM}(t) = U_{\rm c}\sum_{k=-\infty}^{\infty}J_k(\eta)\sin\left[2\pi\left(f_{\rm c} + kf_{\rm m}\right)t + k\varphi_{\rm m} + \varphi_{\rm c}\right], \tag{12}$$

where $J_k(\eta)$ is the Bessel function of first kind with integer order k for the value of η (Fig. 1); $\varphi_{\rm m}$ denotes either $\varphi_{\rm m}^{\rm F}$ or $\varphi_{\rm m}^{\rm P}$. This formula is known as the Chowning relation (Chowning 1973). Although it had been deduced by many different authors formerly,

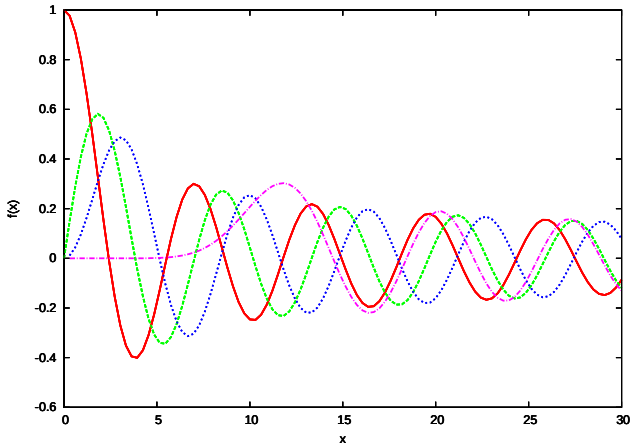

Figure 1. The graph of the first three and the 10th Bessel functions of first kind with integer order k for the value of x. $J_0(x)$ – (red) continuous line, $J_1(x)$ – (green) dashed line, $J_2(x)$ – (blue) dotted line, $J_{10}(x)$ – (purple) dash-dotted line.

Chowning recognized its key role in the electronic sound creation method called FM synthesis.

Similarly to Eq. (4) expression (12) also helps to imagine the spectrum. It is made up of a carrier at f_c and symmetrically placed side peaks separated by f_m. The amplitudes follow the Bessel functions. The behavior of the Bessel functions is well known: except for small arguments ($x < k$), they behave like damped sine functions (see also, Fig. 1). For higher indices the higher order side peaks gradually become more and more important. As a consequence, the amplitude of the central peak gets reduced. The frequency spectrum of an actual FM signal has an infinite number of side peak components, although they become negligibly small beyond a point.

If $|\eta| \ll 1$, we find that $J_0(\eta) \approx 1$, $|J_{\pm1}| = \eta/2$ and $J_k \approx 0$ for $k > 1$. That is, the spectrum can be approximated with an equidistant triplet similarly to AM, but the character of the signal differs from AM: the total amplitude of the modulated wave remains constant. When η increases the amplitude of side peaks also increases, but the Fourier amplitude of the carrier decreases. In other words, the side peaks could be larger than the central peak, on the other hand higher order side frequencies could also be of larger amplitude than the lower order ones.

A more general case is formulated by Schottstaedt (1977)

$$U_\mathrm{FM}(t) = U_\mathrm{c} \sin\left[2\pi f_\mathrm{c} t + \sum_{p=1}^{q} U_\mathrm{m}^{(p)} \sin\left(2\pi f_\mathrm{m}^{(p)} t + \varphi_\mathrm{m}^{(p)}\right) + \varphi_\mathrm{c}\right]$$
$$= U_\mathrm{c} \sum_{k_p=-\infty}^{\infty} \cdots \sum_{k_1=-\infty}^{\infty} \left[\prod_{p=1}^{q} J_{k_p}(U_\mathrm{m}^{(p)})\right] \sin\left[2\pi f_\mathrm{c} t + \sum_{p=1}^{q} k_p \left(2\pi f_\mathrm{m}^{(p)} t + \varphi_\mathrm{m}^{(p)}\right) + \varphi_\mathrm{c}\right]. \quad (13)$$

Here the modulating signal is assumed to be a linear combination of a finite number of sinusoidal functions with arbitrary frequencies $f_\mathrm{m}^{(p)}$, amplitudes $U_\mathrm{m}^{(p)}$ and phases $\varphi_\mathrm{m}^{(p)}$, $p = 1, 2, \ldots, q$. The spectrum contains equidistant frequencies on both sides of the carrier frequency. The amplitudes of the side peaks $f_\mathrm{c} \pm k_p f_\mathrm{m}^{(p)}$ are determined by products of Bessel functions.

2.3 Combined modulation

In practice, the electronic circuits that generate modulated signals generally produce a mixture of amplitude and angle modulations. This combined modulation is disliked in radio techniques but welcomed in sound synthesis and as we will see they appear in the case of Blazhko RR Lyrae stars, as well. Let us overview the basic phenomena of combined modulations following Cartianu (1966). We start with the simplest case: both the AM and FM are sinusoidal and their frequencies are the same.

$$U_\mathrm{Comb}(t) = U_\mathrm{c}\,(1 + h \sin 2\pi f_\mathrm{m} t) \sin\left[2\pi f_\mathrm{c} t + \eta \sin\left(2\pi f_\mathrm{m} t + \phi_\mathrm{m}\right) + \varphi_\mathrm{c}\right]. \quad (14)$$

By suitable choice of the starting epoch, without any restriction of the general validity we can set $\varphi_\mathrm{c} = 0$. Here ϕ_m is the relative phase difference between the modulating FM and AM signals. Other designations are the same as before. The third term of the product (14) is the same as in Eq. (11), therefore, after applying the Chowning relation (12)

$$U_\mathrm{Comb}(t) = U_\mathrm{c}\,(1 + h \sin 2\pi f_\mathrm{m} t) \cdot \sum_{k=-\infty}^{\infty} J_k(\eta) \sin\left[2\pi\left(f_\mathrm{c} + k f_\mathrm{m}\right) t + k\phi_\mathrm{m}\right]. \quad (15)$$

This expression results in an infinite number of amplitude modulated waves. After trigonometrical transformations we get:

$$U_\mathrm{Comb}(t) = U_\mathrm{c} \sum_{k=-\infty}^{\infty} \left\{ J_k(\eta) \sin\left[2\pi\left(f_\mathrm{c} + k f_\mathrm{m}\right) t + k\phi_\mathrm{m}\right] + \frac{h}{2} J_{k-1}(\eta) \sin\left[2\pi\left(f_\mathrm{c} + k f_\mathrm{m}\right) t + (k-1)\,\phi_\mathrm{m} - \frac{\pi}{2}\right] + \frac{h}{2} J_{k+1}(\eta) \sin\left[2\pi\left(f_\mathrm{c} + k f_\mathrm{m}\right) t + (k+1)\,\phi_\mathrm{m} + \frac{\pi}{2}\right] \right\}. \quad (16)$$

It can be seen that each terms consists of three sinusoidal functions with different phases. On the basis of expression (16), the spectrum of combined modulation (14) is comprehensible as a combination of three FM spectra. The peaks are at the same places as the frequencies of the spectrum of (12), but the amplitudes of a pair of side peaks are generally asymmetrical. Using some trigonometrical identities, the rules of summation of parallel harmonic oscillations and relations for Bessel functions we arrive to the expression for the Fourier amplitudes of a certain frequency:

$$A(f_\mathrm{c} + k f_\mathrm{m}) \sim U_\mathrm{c} \left\{ J_k^2(\eta) \left(1 - \frac{hk}{\eta} \sin\phi_\mathrm{m}\right)^2 + \frac{h^2}{4} \cos^2\phi_\mathrm{m} \left[J_{k+1}(\eta) - J_{k-1}(\eta)\right]^2 \right\}^{\frac{1}{2}}, \quad (17)$$

($k = 0, \pm1, \pm2, \ldots$). Introducing the *power difference of the side peaks* as it was done by Szeidl & Jurcsik (2009) $\Delta_l := A^2(f_\mathrm{c} + l f_\mathrm{m}) - A^2(f_\mathrm{c} - l f_\mathrm{m})$, where $l = 1, 2, 3 \ldots$ and taking into account formula (17), we get

$$\Delta_l = -4 \frac{hl}{\eta} U_\mathrm{c}^2 J_l^2(\eta) \sin\phi_\mathrm{m}. \quad (18)$$

This formula is a direct generalisation of the formulae given by Szeidl & Jurcsik (2009) for $l = 1$ and $l = 2$. It is evident, that this asymmetry parameter depends only on ϕ_m, the relative phase of AM and FM. The left hand side peaks are higher than the right hand side ones ($\Delta_l < 0$), if $0 < \phi_\mathrm{m} < \pi$, otherwise the situation is opposite: $\pi < \phi_\mathrm{m} < 2\pi$ and $\Delta_l > 0$. In those very special cases,

where $\phi_{\rm m} = 0$ or $\phi_{\rm m} = \pi$ the side peaks' amplitudes are equal. We have to note that if one of the modulations from AM and FM dominates in the combined case ($h \ll \eta$ or $\eta \ll 1$), the amplitude of the side peaks are almost the same.

3 BLAZHKO MODULATION

RR Lyrae light curves traditionally are described by a Fourier series of a limited number of terms. In Blazhko modulated RR Lyrae stars the sum builds up from terms of harmonics of the main pulsation frequency, side peaks due to the modulation and the modulation frequency and even its harmonics:

$$m(t) = A_0 + \sum_{i=1}^{N} A_i \sin\left[2\pi F_i t + \Phi_i\right], \qquad (19)$$

where either $F_i = jf_0$, ($j = 1, 2, \ldots, n$); or $F_i = kf_{\rm m}$, ($k = 1, 2, \ldots, m$); or $F_i = j'f_0 + k'f_{\rm m}$, ($j' = 1, 2, \ldots, n'$, $k' = 1, 2, \ldots, m'$); $F_i = j''f_0 - k''f_{\rm m}$, ($j'' = 1, 2, \ldots, n''$, $k'' = 1, 2, \ldots, m''$); f_0 and $f_{\rm m}$ are the main pulsation frequency and the modulation one, respectively. The amplitudes A_i and phases Φ_i are considered as independent quantities and determined by a non-linear fit. The necessary number of parameters for a complete light curve solution is $2N + 3$ (amplitudes and phases and two frequencies and the zero point A_0). The number of parameters can be as high as 500-600 for a long time series of good quality (see e.g. Chadid et al. 2010).

In the next subsections we show how the modulation paradigm can be applied and what advantages it has compared to this traditional handling Eq. (19).

3.1 Blazhko stars with AM

To start with, we discuss Blazhko stars' light curves with pure AM effect, although the recent space-born data suggest that all Blazhko RR Lyrae stars show amplitude modulation and simultaneous period changes (Chadid et al. 2010; Benkő et al. 2010; Poretti et al. 2010). We follow a step-by-step generalization process that allows us to separate effects more clearly. We note that the most striking feature of a Blazhko RR Lyrae light curve is the amplitude variation, which is generally easy to find and in many cases the only detectable modulation (see Stothers 2010 and references therein).

To apply the framework described in Sec. 2.1 to an RR Lyrae light curve the course-book formulae need some extensions. We choose a continuous, infinite, periodic function with a non-modulated RR Lyrae shape as a "carrier wave". This function is described by the frequency f_0 and its harmonics, that is $c^*(t) := m(t)$ if $F_i = jf_0$ in Eq. (19).

Although, the exact analytical Fourier spectra of any of the modulated signals discussed in this paper can be calculated without any problems, at least in theory (see also Appendix A), to illustrate the different formulae synthetic light curves and their Fourier spectra were also generated and plotted. An artificial light curve was constructed as a carrier wave with typical RR Lyrae parameters ($f_0 = 2\ {\rm d}^{-1}$ and its 9 harmonics) on a 100 day long time span sampled by 5 min (insert in Fig. 2). The Fourier transform of such a signal is well-known (Fig. 2): it consists of the transformed sinusoidal components given in Eq. A2. (More precisely, due to the finite length of the data set and its sampling, the Fourier transformations should always be multiplied by the Fourier transform of the appropriate window function.)

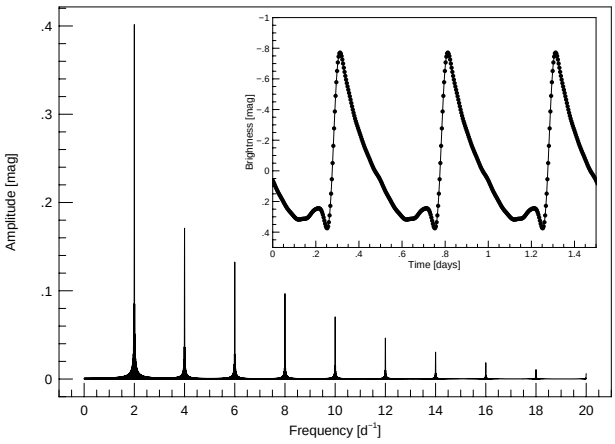

Figure 2. Fourier amplitude spectrum of the artificial RR Lyrae light curve acting as a carrier wave of all modulated light curves constructed in this paper (main panel), and a part of the light curve itself (insert).

Substituting $c^*(t)$ carrier wave into the definition of AM in Eq. (5):

$$m^*_{\rm AM}(t) = \left[1 + \frac{U^*_{\rm m}(t)}{U^*_{\rm c}}\right] c^*(t) = \left[1 + m^*_{\rm m}(t)\right] \left[a_0 + \sum_{j=1}^{n} a_j \sin(2\pi j f_0 t + \varphi_j)\right]. \qquad (20)$$

Expression (20) describes a general amplitude modulated RR Lyrae light curve, $U^*_{\rm m}(t)$ is the modulation signal, $U^*_{\rm c}$ is the amplitude of the non-modulated light curve. On the one hand, the non-zero constant term of a_0 is obligatory from mathematical point of view, otherwise the Fourier sum does not compose a complete set of functions. On the other hand, this value represents the difference between the magnitude and intensity means. More precisely, either we use physical quantities (viz. positive definite fluxes) or we transform normalized fluxes into magnitude scale. In this latter case the average of the transformed light curve differs from zero. In this paper, for traditional purposes we use the second approach. For RR Lyrae stars the typical value of this difference is about some hundredths of a magnitude ($a_0 \ll 1$). It is evident that this constant differs from the zero point of the light curve A_0 given in the apparent magnitude scale.

3.1.1 Sinusoidal amplitude modulation

In the simplest case the modulation is sinusoidal:

$$U^*_{\rm m}(t) = a_{\rm m} \sin(2\pi f_{\rm m} t + \varphi_{\rm m}). \qquad (21)$$

Sample light curves obtained with this assumption from Eq. (20) are shown in Fig. 3. Introducing the modulation depth as $h = a_{\rm m}/U^*_{\rm c}$ the parameters were chosen as $a_0 \leqslant U^*_{\rm c}$ and $a_{\rm m} \leqslant a_0$, resulting in modulations symmetrical to an averaged value viz. a horizontal line (left panels). Right panels show cases with higher modulation depths ($a_{\rm m} > a_0$), where this symmetry is broken. A common feature of these light curves is that the maxima and minima of the envelope curves coincide in time. Furthermore, the average brightness of all light curves vary with $f_{\rm m}$. It can be seen directly from Eq. (20): the $m^*_{\rm m}(t)a_0$ term is responsible for this behaviour. That is, the found mean brightness ($\overline{V}$) variations during

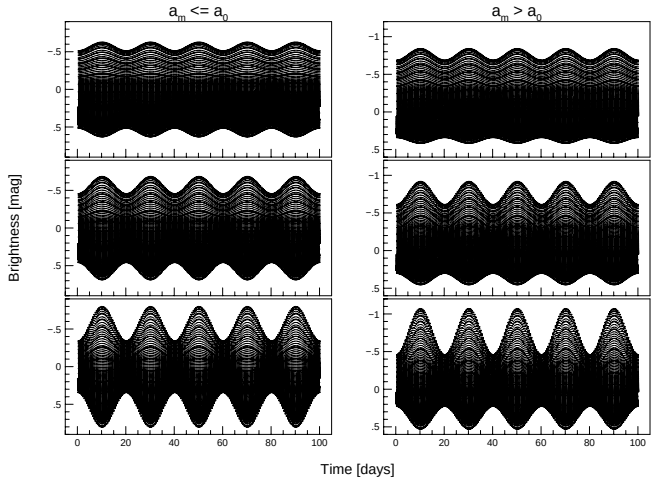

Figure 3. Artificial light curves with a sinusoidal AM computed with the formula Eq. (20). Left panels show symmetrical modulation ($a_\mathrm{m} \leqslant a_0$; $a_0 = 0.2$), the right ones are asymmetrical ($a_\mathrm{m} > a_0$; $a_0 = 0.005$). The modulation depth h is increasing from the top to bottom as $h = 0.1, 0.2, 0.4$; $f_\mathrm{m} = 0.05$ d^{-1} and $\varphi_\mathrm{m} = 270$ deg are fixed.

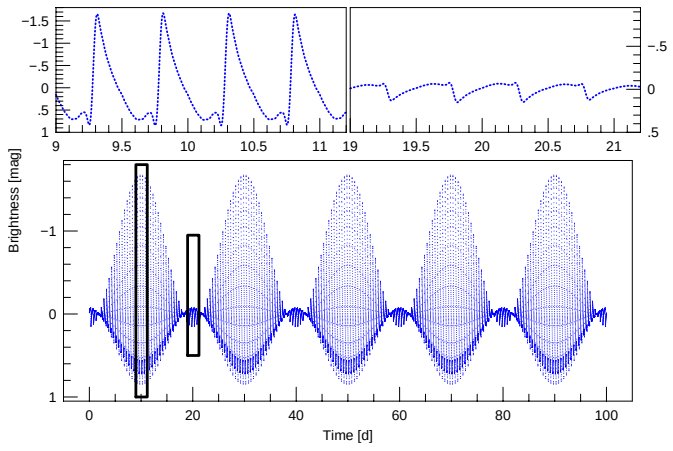

Figure 4. Bottom panel: Artificial light curve with a sinusoidal AM computed with the formula (20). The modulation depth is $h = 1.2$. Other parameters are $a_0 = 0.01$, $f_\mathrm{m} = 0.05$ d^{-1} and $\varphi_\mathrm{m} = 270$ deg. Top panels: Two-day zooms around a maximum (top left) and a minimum (top right) of the modulation cycle.

the Blazhko cycle (Jurcsik et al. 2005) is a natural consequence of the AM.

There is a fascinating case, when the modulation is very strong i.e. when the modulation depth is $h > 1$. Beside the strong light curve changes (Fig. 4) in some Blazhko phases the shape of the light curve looks very unfamiliar (see top right panel in Fig. 4). The relevance of this mathematical case is corroborated by the *Kepler* observation of V445 Lyr that shows similar characteristics (fig 2. in Benkő et al. 2010).

Using some trigonometrical relations, Eq. (20) with (21) can be converted to a handy sinusoidal decomposition form from where the Fourier spectrum is easily seen:

$$m^*_\mathrm{AM}(t) = a_0 + h a_0 \sin\left(2\pi f_\mathrm{m} t + \varphi_\mathrm{m}\right) +$$

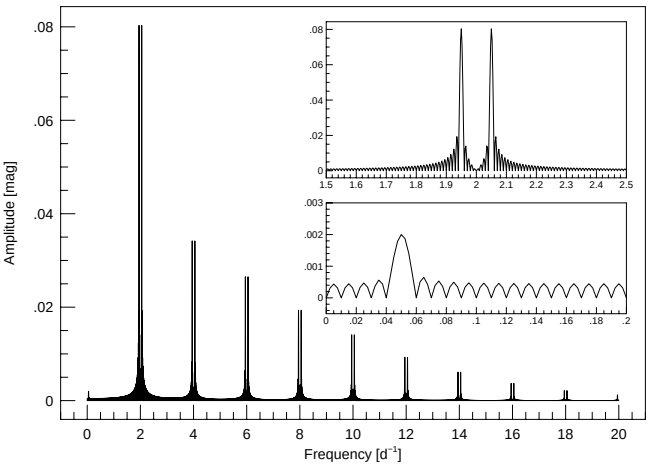

Figure 5. Fourier amplitude spectrum of the artificial sinusoidal AM light curve in bottom right panel of Fig. 3 after the data are prewhitened with the main frequency and its harmonics. Inserts are zooms around the positions of the main frequency $f_0 = 2$ d^{-1} (top), and the modulation frequency $f_\mathrm{m} = 0.05$ d^{-1} (bottom), respectively.

$$\sum_{j=1}^{n} a_j \sin\left(2\pi j f_0 t + \varphi_j\right) +$$

$$\frac{h}{2} \sum_{j=1}^{n} a_j \left\{ \sin\left[2\pi\left(j f_0 - f_\mathrm{m}\right) t + \varphi_j^-\right] + \right.$$

$$\left. \sin\left[2\pi\left(j f_0 + f_\mathrm{m}\right) t + \varphi_j^+\right] \right\}, \quad (22)$$

where $\varphi_j^- = \varphi_j - \varphi_\mathrm{m} + \pi/2$, $\varphi_j^+ = \varphi_j + \varphi_\mathrm{m} - \pi/2$. The Fourier spectrum of such an AM signal is familiar for RR Lyrae stars' experts (see also Fig. 5). It consists of the spectrum of the non-modulated star (third term) as in Fig. 2 and two equidistant side peaks around each harmonic (last term). The amplitudes of the pairs of side peaks are always equal: $A(jf_0 \pm f_\mathrm{m}) \sim a_j h/2$. The second term in Eq. (22), that causes the average brightness variation, produces the frequency f_m itself in the spectrum. The Blazhko modulation frequency is always found in observed data sets extended enough (see e.g. Kovács 1995; Nagy 1998; Jurcsik et al. 2005, 2008; Chadid et al. 2010; Poretti et al. 2010; Kolenberg et al. 2011).

It is a long-standing question whether there is any Blazhko phase where the modulated light curve is identical to the unmodulated one (see Jurcsik, Benkő & Szeidl 2002 and further references therein). In this simplest case the answer is easy. It happens if the second and fourth terms in (22) disappear simultaneously, namely, in the zero points of the modulated sinusoidal function at $t = (k\pi - \varphi_\mathrm{m})/(2\pi f_\mathrm{m})$, k is an arbitrary integer.

The number of used parameters for solving such a light curve (Fig. 3) in the traditional way (according to Eq. 19) is $6n + 5$, where n denote the number of detected harmonics including the main frequency. The necessary number of parameters in our handling is $2n + 5$. The modulation is described by 3 parameters (f_m, a_m, φ_m) as opposed to the traditional framework where this number is $4n + 3$.

3.1.2 Non-sinusoidal AM

As a next step, we assume the modulation function $m^*_{\rm m}(t)$ to be an arbitrary periodic signal represented by a Fourier sum with a constant frequency $f_{\rm m}$. Substituting it into Eq. (20) we get

$$m^*_{\rm AM}(t) = \left[a_0^{\rm A} + \sum_{p=1}^{q} a_p^{\rm A} \sin\left(2\pi p f_{\rm m} t + \varphi_p^{\rm A}\right)\right] c^*(t), \quad (23)$$

where constants are defined by $a_0^{\rm A} = 1 + (a_0^m/U_{\rm c}^*)$, and $a_p^{\rm A} = a_p^m/U_{\rm c}^*$. From now on, the upper index A denotes the AM parameters. Some typical light curves are shown is Fig. 6. It is evident that their envelope curves are non-sinusoidal and their shapes depend on the actual values of $a_p^{\rm A}$ and $\varphi_p^{\rm A}$. The maxima and minima of these envelope curves occur, however, at the same Blazhko phase as in the previous sinusoidal cases. Rewriting of (23) similarly to Eq. (22) but in a more compact form yields

$$m^*_{\rm AM}(t) = \sum_{p=0}^{q}\sum_{j=0}^{n} \frac{a_p^{\rm A}}{2} a_j \sin\left[2\pi\left(j f_0 \pm p f_{\rm m}\right) t + \varphi_{jp}^{\pm}\right], \quad (24)$$

where the two sinusoidal terms appearing analogously to Eq. (22) are formally unified into one formula and denoted by $\pm$ signs; $\varphi_{jp}^{+} = \varphi_j + \varphi_p^{\rm A} - \pi/2$; $\varphi_{jp}^{-} = \varphi_j - \varphi_p^{\rm A} + \pi/2$. The arbitrary constants are chosen to be $\varphi_0^{\rm A} := \varphi_0 := \pi/2$.

By investigating the Fourier amplitude of the side peaks we found that $A(jf_0 \pm pf_{\rm m})/A(jf_0) \sim a_p^{\rm A}$. (i) The amplitude ratio of the side peaks of a given order and the central peak is constant. (ii) The commonly used amplitude ratio $A(jf_0 \pm pf_{\rm m})/A(f_0 \pm pf_{\rm m}) \sim a_j/a_1$ vs. harmonic order is the same as the amplitude ratio of the main frequency $A(jf_0)/A(f_0) \sim a_j/a_1$ vs. harmonic order. (iii) Since the same coefficient $a_p^{\rm A}$ belongs to both side peaks (at $\pm p$), the amplitudes of left-hand-side and right-hand-side peaks are the same. According to this, the generated Fourier spectrum (Fig 7) now shows symmetrical multiplet structure of peaks around the main frequency and its harmonics ($jf_0 \pm pf_{\rm m}$). Each multiplet structure is the same at each harmonic order, that is the number of the side peaks, their frequency differences and amplitude ratios to their central peaks are the same. It is important to note that the number of side peaks (in one side) is equal to p. In addition, the harmonic components of the modulation frequency $pf_{\rm m}$ also appear. (This can be obtained from Eq. (24) if $j = 0$.)

Such a phenomenon was undetected in the observed data of Blazhko stars until recently. Hurta et al. (2008) found equidistant quintuplets in the spectrum of RV UMa for the first time. Besides triplets and quintuplets, sextuplet structures were also found by Jurcsik et al. (2008) in the spectrum of MW Lyr, while Chadid et al. (2010) detected even 8th order (sepdecaplet) multiplet frequencies in the spectrum of *CoRoT* data of V1127 Aql. According to Sec. 2.2, the angle modulations cause infinite numbers of side peaks around each harmonic, therefore, the origin of the observed multiplets as a non-sinusoidal amplitude modulation is certain for those cited cases (e.g. MW Lyr and V1127 Aql), where the harmonics of the modulation frequency are also detected.

In searching for a Blazhko phase where the modulated and carrier waves are identical we concluded that the modulation terms can only be entirely disappearing from the formula (24) if $a_0^{\rm A} = 1$ ($a_0^{\rm m} = 0$) is true, otherwise no such Blazhko phase exists. This necessary condition is complemented by an additional one: the modulation virtually disappears in the moments when $\sum_{p=1}^{q} a_j a_p \sin[2\pi(jf_0 \pm pf_{\rm m})t + \varphi_{jp}^{\mp}] = 0$. The sum has either zero or infinite numbers of zero points depending on the values of the parameters $a_p^{\rm A}$, $\varphi_p^{\rm A}$. That is, generally there are no such phases

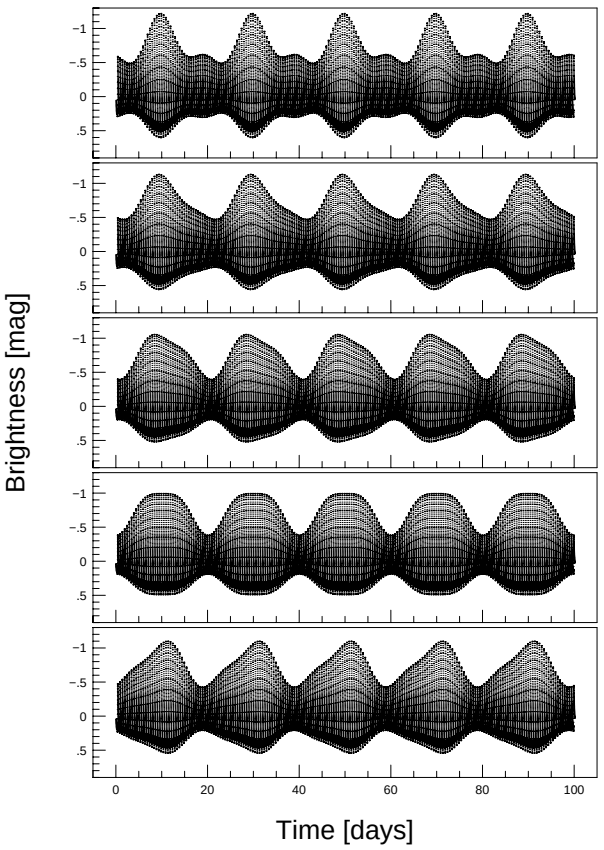

Figure 6. Synthetic light curves of non-sinusoidal AM signals computed by the formula (23). A two-term sum of modulation signal was assumed: $a_1^{\rm A} = 0.01$, $a_2^{\rm A} = 0.2$ mag; $\varphi_1^{\rm A} = 270$ deg are fixed and the phase of the second modulation term varies from top to bottom as: $\varphi_2^{\rm A} = 110$, 140, 220, 270, 360, respectively.

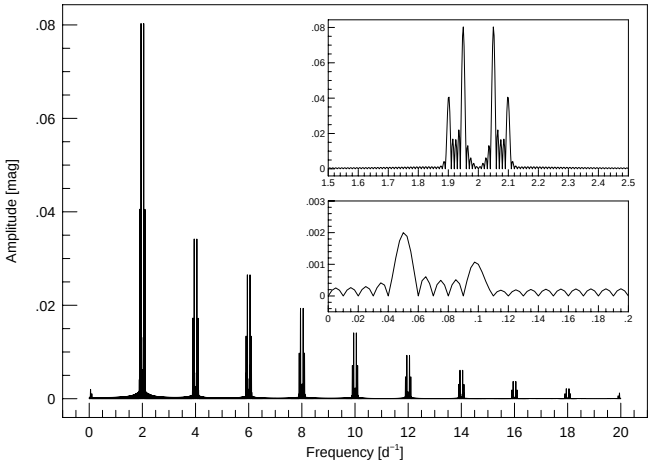

Figure 7. Fourier amplitude spectrum of the synthetic non-sinusoidal AM light curves in Fig. 6 after the data were prewhitened with the main frequency and its harmonics. Inserts are zooms around the positions of the main frequency $f_0 = 2$ d^{-1} (top), and the modulation frequency $f_{\rm m} = 0.05$ d^{-1} (bottom), respectively.

where a non-sinusoidal AM light curve and its carrier wave are identical.

The necessary number of the parameters for a light curve fit of (19) and (23) is $(2q+1)2n+2q+3$ and $2n+2q+3$, respectively. Here n denotes the total number of used harmonics including the main frequency and q is the order of side peak structures as above, (i.e. $q=1$ means triplets, $q=2$ quintuplets, etc). In the traditional description each additional side peak order increased the number of terms by $4n+2$ as opposed to our method, where this increment is only 2.

3.1.3 Parallel AM modulation

Multiperiodic modulation was suspected in XZ Cyg (LaCluyzé et al. 2004), UZ UMa (Sódor et al. 2006), SU Col (Szczygieł & Fabrycky 2007), and LS Her (Wils, Kleidis & Broens 2008). The Blazhko RR Lyrae stars of the MACHO and OGLE surveys (Alcock et al. 2000; Moskalik & Poretti 2003) that have unequally spaced triplet structures in their Fourier spectra are possibly also multiperiodically modulated variables. CZ Lac (Sódor et al. 2011) is the first Blazhko star with multiperiodic modulation where both modulation periods are identified. Not only modulation side peaks but linear combinations of the modulation frequencies also appear. Signs of multiple modulation were discovered in *Kepler* data of V445 Lyr (Benkő et al. 2010). There are numerous possibilities for creating a multiply modulated light curve. Let us review some of them.

The most simple case is a natural generalization of Eq. (23) when the modulation signal is assumed to be a sum of signals with different $\hat{f}_{\rm m}^r$, where $r=1,2,\ldots$ signs constant frequencies. Let signals be independent, i.e., the modulation signal consists of linearly superimposed waves. In this case, Eq. (23) reads as:

$$m^*_{\rm AM}(t)=\left[\hat{a}_0+\sum_{r=1}^{s}\sum_{p=1}^{q_r}\hat{a}_{pr}\sin\left(2\pi p\hat{f}_{\rm m}^r t+\hat{\varphi}_{pr}\right)\right]c^*(t), \tag{25}$$

where $\hat{a}_0=1+\sum_{r=1}^{s}a_{0r}^m/U_{\rm c}^*$, and $\hat{a}_{pr}=a_{pr}^m/U_{\rm c}^*$. This formula is demonstrated in Fig. 8. In this figure, only two modulation waves are taken into account and the only varied parameter is the frequency of the second modulation is $\hat{f}_{\rm m}^2$. When the two modulation frequencies are comparable ($\hat{f}_{\rm m}^1=0.1$ d^{-1} and $\hat{f}_{\rm m}^2=0.09$ d^{-1} in panel a the envelope shape of the light curve shows the well-known beating phenomenon. Here the beating period is 200 days, albeit the modulation periods are close to the shortest known ones. It is easy to understand that the observations taken on a moderate time span often detect only the gradual increase or decrease of the amplitude of the Blazhko cycles. In panel b of Fig. 8 $\hat{f}_{\rm m}^2$ was set to 0.075 d^{-1}, that is the ratio of the modulation frequencies is 4:3, similarly to the case of CZ Lac during its second observed season in Sódor et al. (2011). The amplitude changes of the consecutive Blazhko cycles need well-covered long-term time series observations, otherwise the interpretation becomes difficult. Panel c in Fig. 8 shows the case where the frequency of the second modulation is half of the first one ($\hat{f}_{\rm m}^2=0.05$ d^{-1}). These specially selected values cause alternating higher and lower Blazhko cycles. The exact 2:1 ratio between the two modulation frequencies leads to the same result as a two-term non-sinusoidal modulation in Eq. (23) (see also top panel in Fig. 6). The bottom panel in Fig. 8 shows a case where the second modulation has a much longer period than the primary Blazhko cycle. In a first inspection the top and bottom panels are very similar apart from a phase shift.

To reveal the real situation we need to compare their Fourier

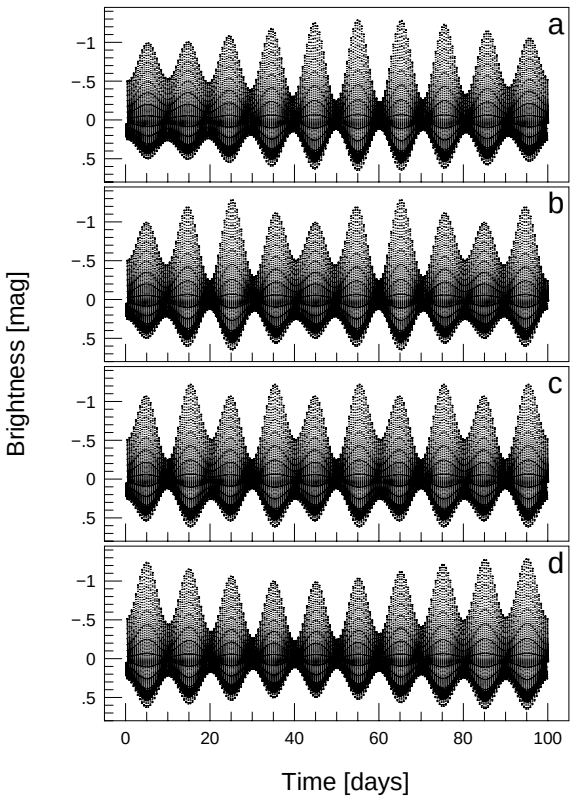

Figure 8. Artificial light curves calculated with two independent sinusoidal AM modulations according to the formula of (25). The fixed parameters were $a_0=0.01$, $\hat{a}_{11}=0.5$, $\hat{a}_{12}=0.2$ mag, $\hat{f}_{\rm m}^1=0.1$ d^{-1}, $\hat{\varphi}_{11}=270$, $\hat{\varphi}_{12}=120$ deg, where $\hat{f}_{\rm m}^2$ changes from top to bottom as 0.09, 0.075, 0.05 and 0.01 d^{-1}, respectively.

spectra starting with

$$m^*_{\rm AM}(t)=\sum_{r=1}^{s}\sum_{p=0}^{q_r}\sum_{j=0}^{n}\frac{\hat{a}_{pr}}{2}a_j\sin\left[2\pi\left(jf_0\pm p\hat{f}_{\rm m}^r\right)t+\hat{\varphi}_{jpr}^{\pm}\right]. \tag{26}$$

Where the constants are chosen similarly to (24): $\hat{\varphi}_{jpr}^{-}=\varphi_j-\hat{\varphi}_{pr}+\pi/2$; $\hat{\varphi}_{jpr}^{+}=\varphi_j+\hat{\varphi}_{pr}-\pi/2$; $\varphi_0=\hat{\varphi}_{0r}=\pi/2$. It is easy to see that the Fourier spectrum of expression (26) contains s sets of side peaks shown in Fig. 7. The qualitative structure of these sets is the same. It consists of the carrier's spectrum (jf_0), the peaks of the different modulation frequencies and their harmonics ($p\hat{f}_{\rm m}^r$), and the side peaks around the main frequency and its harmonics: $jf_0\pm p\hat{f}_{\rm m}^r$, where $p=1,2,\ldots,q_r$, and $r=1,2,\ldots,s$. Due to the independence of the modulation waves no further side peaks appear.

3.1.4 Modulated modulation – the AM cascade

It is hard to imagine, however, that in a real stars's case, the different modulating waves are independently superimposed without any interactions. Let us investigate the possibility of the modulated modulation: the cascade. In other words, the modulation signal is composed of recursively modulated waves as

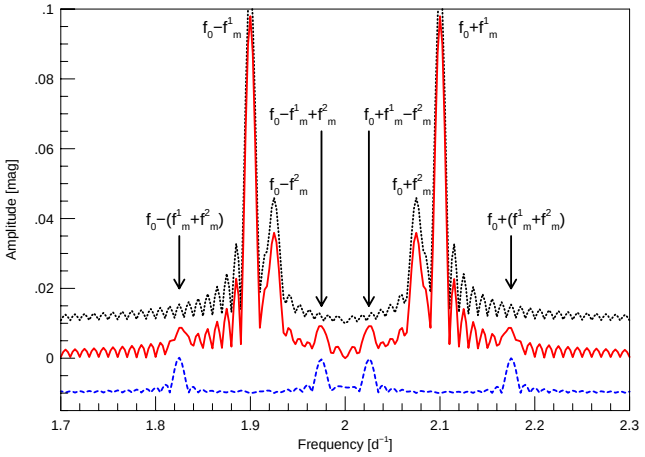

Figure 9. Fourier amplitude spectra of the artificial cascade AM light curves with parameters of panel b in Fig. 8 – (black) dotted line – and its cascade equivalent – (red) continuous line. The spectra show the interval around the main pulsation frequency after the data are prewhitened with it. The (blue) dashed line shows the spectrum of cascade case after the side peaks $f_0 \pm f_{\rm m}^1$, $f_0 \pm f_{\rm m}^2$ are also removed (for better visibility the top and bottom spectra are shifted with +0.01 and −0.01 mag, respectively).

$$
\begin{aligned}
c^{(1)}(t) &:= c^*(t), \;\; m_{\rm m}^{(1)}(t) = m_{\rm m}^*(t), \\
c^{(2)}(t) &:= m_{\rm AM}^{(1)}(t) = [1 + m_{\rm m}^{(1)}(t)]c^{(1)}(t), \\
& \quad\; m_{\rm AM}^{(2)}(t) = [1 + m_{\rm m}^{(2)}(t)]c^{(2)}(t), \ldots, \\
& \quad\; m_{\rm AM}^{(s)}(t) = [1 + m_{\rm m}^{(s)}(t)]c^{(s)}(t). \qquad (27)
\end{aligned}
$$

$$
m_{\rm AM}^*(t) = \prod_{r=1}^{s} \left[\tilde{a}_{0r} + \sum_{p=1}^{q_r} \tilde{a}_{pr} \sin\left(2\pi p \tilde{f}_{\rm m}^r t + \tilde{\varphi}_{pr}\right) \right] c^*(t), \qquad (28)
$$

where $\tilde{a}_{0r} = 1 + a_{0r}^m / U_{cr}^*$, $\tilde{a}_{pr} = a_{pr}^m / U_{cr}^*$. U_{cr}^* denotes the amplitude of the rth carrier wave $c^{(r)}(t)$. On the basis of a visual inspection, there are imperceptible differences among the light curves produced by this expression (28) and those that can be seen in Fig. 8. The Fourier spectrum, however, contains additional peaks at the linear combinations of f_0 and $\tilde{f}_{\rm m}^r$ as it is shown in Fig 9. To understand this spectrum we generate Eq. (28) in a form similar to Eq. (26).

$$
\begin{aligned}
m_{\rm AM}^*(t) = \sum_{r=1}^{s} \sum_{p=0}^{q_r} \sum_{j=0}^{n} \frac{1}{2} \left(\prod_{\substack{r'=1 \\ r' \neq r}}^{s} \tilde{a}_{0r'} \right) \tilde{a}_{pr} a_j \cdot \\
\sin\left[2\pi \left(j f_0 \pm p \tilde{f}_{\rm m}^r \right) t + \tilde{\varphi}_{jpr}^{\pm} \right] + \\
\sum_{k=2}^{s} \sum_{r \in \mathcal{R}_k} \sum_{p=1}^{q_r} a_0 \prod_{r' \in \mathcal{R}_k^{\rm C}} \tilde{a}_{0r'} \left(\prod_{r} \tilde{a}_{pr} \right) \mathcal{S}_k(\boldsymbol{\alpha}) + \\
\sum_{k=2}^{s} \sum_{r \in \mathcal{R}_k} \sum_{p=1}^{q_r} \sum_{j=1}^{n} a_j \prod_{r' \in \mathcal{R}_k^{\rm C}} \tilde{a}_{0r'} \left(\prod_{r} \tilde{a}_{pr} \right) \mathcal{S}_{k+1}(\boldsymbol{\beta}), \qquad (29)
\end{aligned}
$$

$\tilde{\varphi}_{jpr}^{-} = \varphi_j - \tilde{\varphi}_{pr} + \pi/2$; $\tilde{\varphi}_{jpr}^{+} = \varphi_j + \tilde{\varphi}_{pr} - \pi/2$; $\tilde{\varphi}_{0r} = \pi/2$. An index set $\mathcal{R}_s$ is defined so that it contains all r indices from $r = 1, 2, \ldots, s$. Index sets $\mathcal{R}_k$ means all subsets of $\mathcal{R}_s$ what contains k elements. Therefore, the total number of $\mathcal{R}_k$ sets is $\binom{s}{k}$. The sums over $r \in \mathcal{R}_k$ mean a sum over the all possible combinations of the k number of different indices r. Similarly r' always runs over the complement of a set $\mathcal{R}_k^{\rm C}$ of the actual $\mathcal{R}_k$. The functions $\mathcal{S}_k$ build up sums of sinusoidal functions (see for the definition and further details in Appendix B) of the linear combinations of k angles. Here the components of the $\boldsymbol{\alpha}$ and $\boldsymbol{\beta}$ vectors are $\alpha_r = 2\pi p \tilde{f}_{\rm m}^r t + \tilde{\varphi}_{pr}$, $r \in \mathcal{R}_k$, $\beta_{k+1} = 2\pi j f_0 t + \varphi_j$ and $\beta_r = \alpha_r$.

For better comparison we present the formula in the form of Eq. (29) instead of the most possible compact one. Although Eq. (29) seems to be complicated, the meaning of each term is simple: the first term can be directly compared to the linearly superimposed case Eq. (26). It produces all the peaks in the Fourier spectrum appearing in that case: the main pulsation frequency and its harmonics jf_0, modulation frequencies and its harmonics $p\tilde{f}_{\rm m}^r$, the side frequencies around the main frequency and its harmonics ($jf_0 \pm p\tilde{f}_{\rm m}^r$). The second sum in Eq. (29) belongs to the peaks of all the possible linear combinations of $p\tilde{f}_{\rm m}^r$, whilst the last term is responsible for the many linear combination frequencies around the main frequency and its harmonics (Fig. 9). The latter two types of combination terms were detected by Sódor et al. (2011) in the Fourier spectrum of CZ Lac, the only well-studied multiply modulated RR Lyrae star.

Long-term secondary changes in Blazhko cycles can be explained by the variable strength of the modulation. To formulate this assumption we arrived at

$$
m_{\rm AM}^*(t) = \left\{ 1 + \left[1 + m_{\rm m}'(t) \right] m_{\rm m}''(t) \right\} c^*(t) \qquad (30)
$$

The formula (30) can be considered as a special case of (28) when $s = 2$ and $\tilde{a}_{01} = 0$.

3.2 Blazhko stars with FM

We remind the reader of the possible absence of real Blazhko stars with pure AM that was mentioned in the introductory paragraphs of Sec. 3.1. The only difference between pure AM and FM cases is that RR Lyrae stars showing pure PM/FM are much more rarely reported than pure AM ones, but there are some examples (e.g. Kurtz et al. 2000; Derekas et al. 2004).

How can the formalism discussed in Sec. 2.2 be applied to RR Lyrae stars? Let us assume the same carrier wave as in the case of AM, but here the instantaneous frequency $f(t)$ is denoted as $f_0 + m_{\rm m}^*(t)$, and $m_{\rm m}^*(t)$ is an arbitrary (bounded) modulation signal.

$$
m_{\rm FM}^*(t) = a_0 + \sum_{j=1}^{n} a_j \sin\left\{ 2\pi j \left[f_0 + m_{\rm m}^*(t) \right] t + \varphi_j \right\}. \qquad (31)
$$

Expression (31) describes a general frequency modulated RR Lyrae light curve.

3.2.1 The sinusoidal FM

When the modulating function is sinusoidal and expressed in the same form as (21), Eq. (31) becomes

$$
\begin{aligned}
m_{\rm FM}^*(t) &= a_0 + \\
&\sum_{j=1}^{n} a_j \sin\left[2\pi j f_0 t + j a^{\rm F} \sin\left(2\pi f_{\rm m} t + \varphi^{\rm F} \right) + \varphi_j \right], \qquad (32)
\end{aligned}
$$

where $a^{\rm F} = a_{\rm m}/f_{\rm m}$, $\varphi^{\rm F} = \varphi_{\rm m} + \pi/2$ and the upper index F marks the parameters of FM. The amplitude of this signal is determined by the Fourier amplitudes a_j of the carrier signal, hence no amplitude changes are present. In the bottom panel of Fig. 10 a simulated light

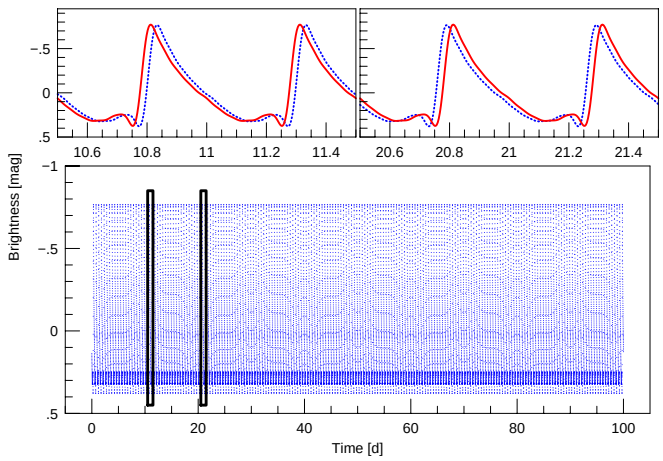

Figure 10. Bottom: Artificial FM light curve produced with sinusoidal modulation according to Eq. (32). Fourier parameters of the "carrier light curve" are the same as before, $a^{\rm F} = 0.279; \varphi^{\rm F} = 0$. Boxes show the locations of the top panels. Top panels: One-day zooms from two different phases of the modulation cycle. The non-modulated "carrier" light curve is shown by a (red) continuous lines while (blue) dotted lines denotes FM signal. The periodic phase shift (viz. PM) caused by FM can be clearly identified.

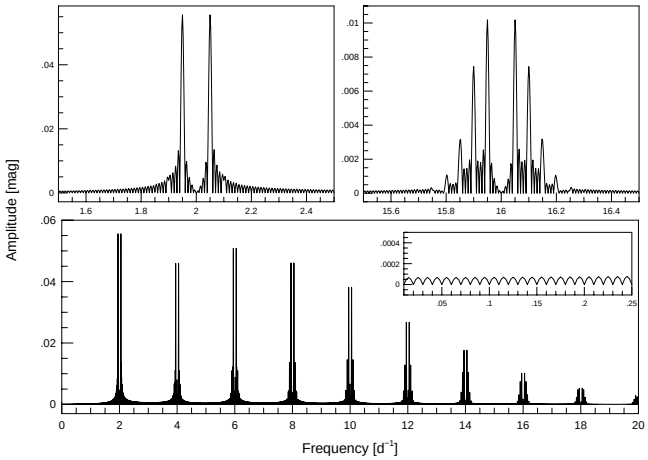

Figure 11. Bottom: Fourier amplitude spectrum of the artificial sinusoidal FM light curve in Fig. 10 after the data are prewhitened with the main frequency and its harmonics. Top panels are zooms around the positions of the main frequency $f_0 = 2\,{\rm d}^{-1}$ (top left), and its 7th harmonics $8f_0 = 16\,{\rm d}^{-1}$ (top right), respectively. The modulation frequency f_m is missing from the spectrum (insert).

curve is shown. It is evident that there is no amplitude change. Two-day zooms from two different phases of the modulation cycle are shown in the top panels. The periodic phase shift caused by FM can be identified well: in the left-hand-side panel the non-modulated light curve is to the left from the FM light curve whilst in the right-hand side panel the situation is opposite.

Using Chowning's relation (12) we get from (32):

$$m^*_{\rm FM}(t) = a_0 + \sum_{j=1}^{n}\sum_{k=-\infty}^{\infty} a_j J_k\left(ja^{\rm F}\right) \sin\left[2\pi\left(jf_0 + kf_{\rm m}\right)t + k\varphi^{\rm F} + \varphi_j\right]. \quad (33)$$

This equation shows the main characteristics of the Fourier spectrum (Fig. 11). It consists of peaks at f_0 and at its harmonics jf_0 and each of them is surrounded by side peaks at $jf_0 \pm kf_{\rm m}$ with symmetrical amplitudes at the two sides. This symmetry of the amplitudes can be seen from the expression of amplitude ratio $A(jf_0 \pm kf_{\rm m})/A(jf_0) \sim |J_{\pm k}(ja^{\rm F})|$, and it is known that $J_{-k}(z) = (-1)^k J_k(z)$. It is worth to compare the AM spectra in Figs. 5 and 7 to this FM spectrum. The Fourier amplitude of the side peaks are proportional to the Bessel function, and an immediate consequence can be seen in the figure: the amplitude of the triplet peaks are higher at $3f_0$ than at $2f_0$. (Although it is not shown in the figure, the higher order $j > 5$ harmonics have also smaller amplitudes than their side frequencies' ones.) Since the argument of the Bessel functions depends on the order of harmonics j, higher order harmonics "feel" larger modulation index, which results in more side peaks around the higher order harmonics (see inserts in Fig. 11). This effect was found for V1127 Aql from its *CoRoT* data by Chadid et al. (2010). A further remarkable flavour of this Fourier spectrum is, that it does not include $f_{\rm m}$ as opposed to any of the AM spectra (insert in Fig. 11).

Let us return to the question whether there is any phase in the modulation cycle where the light curve is identical to the monoperiodic light curve (carrier signal). As it was shown in the case of sinusoidal AM modulation, there are some such possible phases. Looking at the formula (32) it can be realised that the modulation disappears at the moments of time if $t = (l\pi - \varphi^{\rm F})/(2\pi f_{\rm m})$, where l is an arbitrary integer.

Estimating the number of the necessary parameters for a light curve fit the traditional description Eq. (19) needs $\approx 2n + 3 + 4\sum_{j=1}^{n}[{\rm int}(ja^{\rm F}) + 1]$, where "int" means the integer function, and n is the number of all harmonics including the main frequency as well. At the same time, Eq. (32) requires only $2n+5$ parameters, no more than in the sinusoidal AM case. For a typical case plotted in Fig. 10 ($n = 10$ and $a^{\rm F} = 0.27$), the difference is 143 parameters versus 25.

3.2.2 *The case of non-sinusoidal FM*

Assuming an arbitrary periodic modulation with a fixed frequency we substitute a Fourier sum representing this modulation signal into Eq. (31) and get

$$m^*_{\rm FM}(t) = a_0 + \sum_{j=1}^{n} a_j \sin\left[2\pi j f_0 t + j\sum_{p=1}^{q} a_p^{\rm F} \sin\left(2\pi p f_{\rm m} t + \varphi_p^{\rm F}\right) + \phi_j\right], \quad (34)$$

where the constant terms are contracted as $\phi_j = ja_0^{\rm F} + \varphi_j$. As in the previous sinusoidal case the equation can be rewritten as

$$m^*_{\rm FM}(t) = a_0 + \sum_{j=1}^{n}\sum_{k_1,k_2,\ldots,k_p=-\infty}^{\infty} a_j \left[\prod_{p=1}^{q} J_{k_p}(ja_p^{\rm F})\right] \cdot \sin\left[2\pi\left(jf_0 + \sum_{p=1}^{q} k_p p f_{\rm m}\right)t + \sum_{p=1}^{q} k_p\varphi_p^{\rm F} + \phi_j\right]. \quad (35)$$

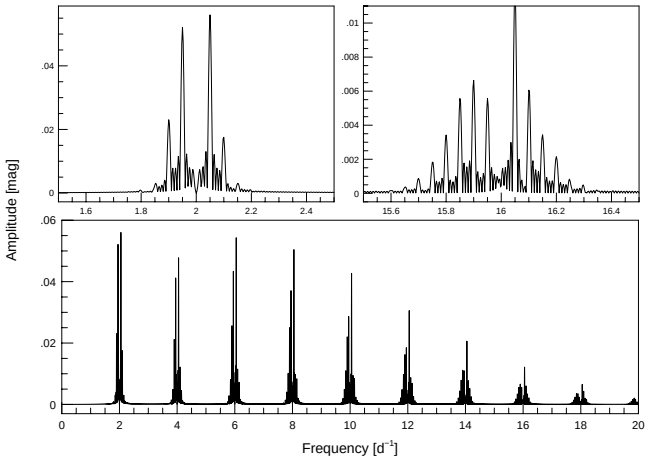

Figure 12. Bottom: Fourier amplitude spectrum of an artificial non-sinusoidal FM light curve calculated by the formula of (34) after the data are prewhitened with the main frequency and its harmonics. Parameters of the generated light curve were the same as for the light curve in Fig. 10, and $p = 2$, $a_2^{\rm F} = -0.1$ mag, $\varphi_2^{\rm F} = \pi/4$. Top panels are zooms around the positions of the main frequency $f_0 = 2\,{\rm d}^{-1}$ (top left), and its 7th harmonic $8f_0 = 16\,{\rm d}^{-1}$ (top right), respectively.

In one sense, this formula is a generalisation of (13) to the case for a non-sinusoidal carrier wave, in the other sense however, the modulation frequencies are chosen specially as $f_{\rm m}^p := pf_{\rm m}$.

Comparing equation (35) with (33) it can be realised that the structure of both Fourier amplitude spectra should be similar (cf. also Fig. 11 and Fig. 12), although there are significant differences, as well. First of all, besides the same values of common Fourier parameters of a sinusoidal and a non-sinusoidal case, the detectable side peaks are more numerous than for the non-sinusoidal case. The reason is simple: the higher order terms in the modulation signals' sum increase the "effective modulation index". The most noteworthy difference is the disappearance of the symmetry between the amplitude of the side peaks from the lower and higher frequency parts.

To understand this let us investigate the simplest non-sinusoidal case, if $q = 2$ and concentrate only on the side peaks around the main pulsation frequency ($j = 1$). Then the above expression (35) is simplified to

$$\sum_{k_1=-\infty}^{\infty}\sum_{k_2=-\infty}^{\infty} a_1 J_{k_1}(a_1^{\rm F}) J_{k_2}(a_2^{\rm F}) \cdot \sin\left\{2\pi\left[f_0 + (k_1+2k_2)\,f_{\rm m}\right]t + k_1\varphi_1^{\rm F} + k_2\varphi_2^{\rm F} + \phi_1\right\}. \quad (36)$$

For calculating the amplitude of the triplet's side peaks $A(f_0 \pm f_{\rm m})$ we have to sort out the corresponding terms from the above infinite sum such as $k_1 = 1 - 2k_2$ and $k_1 = -(2k_2+1)$, for the right-hand-side and left-hand-side peaks, respectively (k_2 is an arbitrary integer). It can be seen, that both sums include the same elements, because $J_{-3}(a_1^{\rm F})J_1(a_2^{\rm F}) = J_3(a_1^{\rm F})J_{-1}(a_2^{\rm F})$, $J_{-5}(a_1^{\rm F})J_2(a_2^{\rm F}) = J_5(a_1^{\rm F})J_{-2}(a_2^{\rm F}), \ldots$ for each pair and the relative phase differences have the same values with an opposite sign. The only differing terms contain $J_1(a_1^{\rm F})J_0(a_2^{\rm F})$ in the sum of $A(f_0 + f_{\rm m})$ and $J_{-1}(a_1^{\rm F})J_0(a_2^{\rm F})$ in the sum of $A(f_0 - f_{\rm m})$. These terms are responsible for the asymmetry of the side peaks. Introducing power

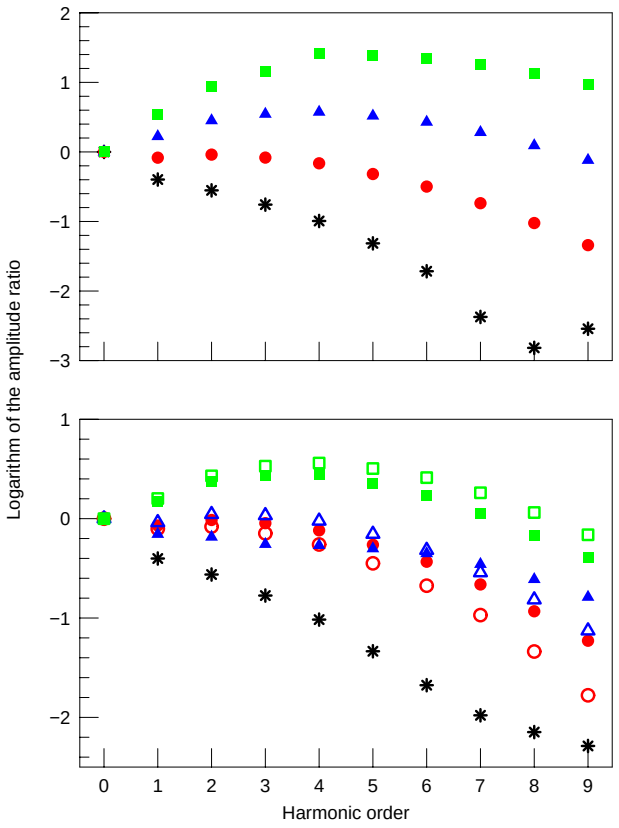

Figure 13. Amplitude ratios of the harmonic components of the main pulsation ($A(jf_0)/A(f_0)$) plotted on decimal logarithmic scale compared to the amplitude ratios of the modulation components: $A(jf_0+pf_{\rm m})/A(f_0+pf_{\rm m})$. Top: sinusoidal FM case; $p = 0$, 1, 2 and 3 (black) asterisks, (red) circles, (blue) triangles and (green) squares, respectively. Bottom: non-sinusoidal FM; shape of the symbols denotes p as in the top panel, but filled symbols mark positive ps (higher frequency side peaks) while the open symbols show negative ps (lower frequency side peaks).

difference of the side peaks as in Sec. 2.3 we get

$$\Delta_1 = 4\hat{A}_1 J_1(a_1^{\rm F}) J_0(a_2^{\rm F}) \cos(\hat{\Phi}_1 - \varphi_1^{\rm F}). \quad (37)$$

Here $\hat{A}_1$ and $\hat{\Phi}_1$ indicate the amplitude and phase of a sinusoidal oscillation obtained by summing all the terms in (36) except the different ones. The asymmetry of the higher order side peaks ($|k_1 + 2k_2| > 1$) can be verified in a similar manner.

This asymmetry has a further consequence. The functions of amplitude ratio vs. harmonic orders belonging to a given pair of side peaks are diverge from each other (Fig. 13). This behaviour is well-known from the similar diagrams of observed Blazhko RR Lyrae stars (Jurcsik et al. 2009b; Chadid et al. 2010; Kolenberg et al. 2011). It can also be seen that the actual character of the asymmetry can change with the harmonic order j or even within a given order with the different p. For example, in Fig. 13 if $p = 1$ (triplets), the right-hand-side peaks are always higher than the left-hand-side ones and the difference between the pairs are increasing with harmonic orders. Meanwhile, if $p = 3$ (septuplets) the situation is the opposite. In the case of $p = 2$ (quintuplets) the lower frequency peaks have higher amplitude around the lower or-

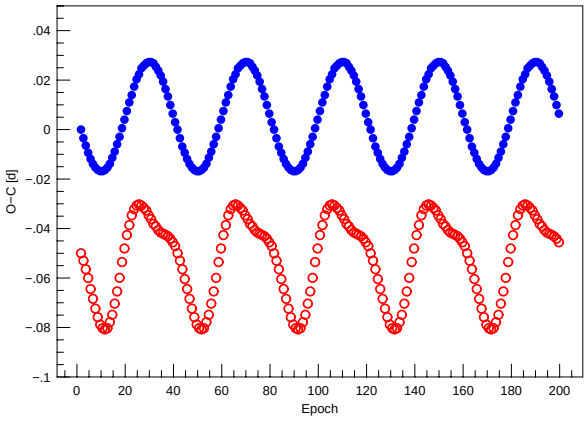

Figure 14. O-C diagram of the maxima of FM light curves with sinusoidal – (blue) filled circles – and non-sinusoidal – (red) empty circles – modulations, respectively. The input light curves are generated from the formulae of (32) and (34) with the same parameters as the light curve shown in Fig. 10 (sinusoidal case) and Fourier plot in Fig. 12 (non-sinusoidal case). (For better visibility the non-sinusoidal curve is shifted by -0.05.)

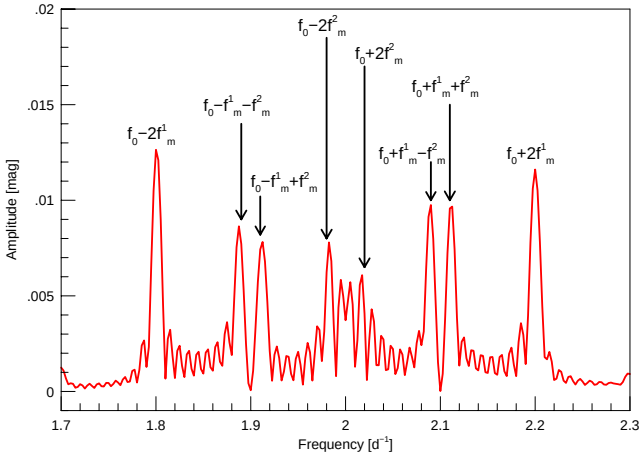

Figure 15. Fourier amplitude spectra of the artificial light curves containing two parallel FM modulations in formula (38). The figure shows a zoom around the main pulsation frequency after the data are prewhitened with it and the triplet components $f_0 \pm \hat{f}^1_{\rm m}$, $f_0 \pm \hat{f}^2_{\rm m}$. The highest peaks are at the quintuplet frequencies ($f_0 \pm 2\hat{f}^1_{\rm m}$, $f_0 \pm 2\hat{f}^2_{\rm m}$) and at the linear combination frequencies. (The used parameters are: $\hat{f}^1_{\rm m} = 0.1$ d^{-1}, $\hat{f}^2_{\rm m} = 0.01$ d^{-1}, $\hat{a}^{\rm F}_{11} = 0.5$ mag, $\hat{a}^{\rm F}_{12} = 0.2$ mag.)

der ($j < 5$) harmonics, for higher harmonics ($j > 7$) the amplitude ratios of the pairs of side peaks reversed.

As it was discussed in the introductory Section 2.3 simultaneous and sinusoidal amplitude and phase modulations result in an asymmetrical spectrum, therefore, the asymmetry of the amplitude spectrum alone is not a good criterion for detecting a non-sinusoidal FM. The classical O−C diagram is an ideal tool for this purpose (see e.g. Sterken 2005). Fig. 14 illustrates the O−C diagrams of the maxima for two artificial FM light curves: a sinusoidal and a simple non-sinusoidal one.

At the end of this section we compare the necessary parameters of a potential fit based on the classical description (19) and the present (31) one. In the latter case this value is $2n + 2q + 3$, where n and q are defined in (31). The expression is the same as in the case of a non-sinusoidal AM. The traditional formula needs $\approx 2n + 3 + (4\sum_{j=1}^{n}[\mathrm{int}(j\sum_{p=1}^{q} a_p^{\rm F}) + 1])$ parameters. For the case showed in Fig. 12 ($n = 10$, $a_1^{\rm F} = 0.27$, $a_2^{\rm F} = 0.1$) these values are 27 and 163, respectively.

3.2.3 *Parallel FM*

We continue the discussion as in the case of AM. The next step is the multiply modulated FM with independently superimposed modulation signals (parallel modulation). As has already been noted, the chance of such a scenario is very low for stars, but this case shows a new phenomenon, which is why it is worth to have a look at it.

$$\hat{m}^*_{\rm FM}(t) = a_0 + \sum_{j=1}^{n} a_j \sin\left\{2\pi j f_0 t + j\left[\sum_{r=1}^{s}\sum_{p=1}^{q_r} \hat{a}^{\rm F}_{pr} \sin\left(2\pi p \hat{f}^r_{\rm m} t + \hat{\varphi}^{\rm F}_{pr}\right)\right] + \hat{\phi}_j\right\}. \quad (38)$$

Here $\hat{\phi}_j := j\hat{a}^{\rm F}_{0r} + \varphi_j$. The formula (38) can easily be transformed with the help of Eqs. (13) and (35) to

$$\hat{m}^*_{\rm FM}(t) = a_0 + \sum_{j=1}^{n} \sum_{k_{11},k_{12},\ldots,k_{q_s s}=-\infty}^{\infty} a_j \left[\prod_{r=1}^{s}\prod_{p=1}^{q_r} J_{k_{pr}}(j\hat{a}^{\rm F}_{pr})\right] \cdot \sin\left[2\pi\left(j f_0 + \sum_{r=1}^{s}\sum_{p=1}^{q_r} k_{pr} p \hat{f}^r_{\rm m}\right) t + \sum_{r=1}^{s}\sum_{p=1}^{q_r} k_{pr}\hat{\varphi}^{\rm F}_{pr} + \hat{\phi}_j\right]. \quad (39)$$

There is a fundamental difference between the construction of Fourier spectra of parallel AM and FM signals. While the AM spectra build up from a simple sum of the component spectra belonging to a given modulation frequency $\hat{f}^r_{\rm m}$, FM spectra contain all possible linear combinations of $\hat{f}^r_{\rm m}$ and the harmonics of the main pulsation frequency jf_0. This is illustrated in Fig. 15. In practice, this effect complicates distinguishing Fourier spectra from the cascade AM and parallel FM.

3.2.4 *The FM cascade*

Although a parallel FM modulation results in a more complex Fourier spectrum than either a parallel or even a cascade AM, our former statement is still true. There is a very low chance for independently superimposed modulation signals in real stars. Let us turn to the FM cascade (viz. the modulated modulation) case now!

$$\tilde{m}^*_{\rm FM}(t) = a_0 + \sum_{j=1}^{n} a_j \sin\left[2\pi j f_0 t + j\tilde{C}_{\rm FM}(t) + \tilde{\phi}_j\right], \quad (40)$$

where

$$\tilde{C}_{\rm FM}(t) := m^{(1)}_{\rm FM}(t) = \sum_{p=1}^{q_1} \tilde{a}^{\rm F}_{p1} \sin\left[2\pi p \tilde{f}^1_{\rm m} t + p m^{(2)}_{\rm FM}(t) + \tilde{\varphi}^{\rm F}_{p1}\right],$$

$$m^{(2)}_{\rm FM}(t) = \sum_{p=1}^{q_2} \tilde{a}^{\rm F}_{p2} \sin\left[2\pi p \tilde{f}^2_{\rm m} t + p m^{(3)}_{\rm FM}(t) + \tilde{\varphi}^{\rm F}_{p2}\right], \ldots,$$

$$m^{(s)}_{\rm FM}(t) = \sum_{p=1}^{q_s} \tilde{a}^{\rm F}_{ps} \sin\left(2\pi p \tilde{f}^s_{\rm m} t + \tilde{\varphi}^{\rm F}_{ps}\right), \quad (41)$$

and $\tilde{\phi}_j = j\tilde{a}_{01}^{\rm F} + \varphi_j$. As we can see, the function $\tilde{C}_{\rm FM}(t)$ consists of a modulation cascade with s elements, where all elemental modulation functions $m_{\rm FM}^{(r)}(t)$ are represented by finite Fourier sums. That is, they are assumed to be independent periodic signals with the frequencies $\tilde{f}_{\rm m}^r$. Since an FM modulation can be reproduced by infinite series of sinusoidal functions (see Chowning relation), it is not a surprise that the sinusoidal decomposition of the expression (40) is very similar to the parallel case (39). Namely

$$\tilde{m}_{\rm FM}^*(t) = a_0 + \sum_{j=1}^{n} \sum_{k_{11},k_{12},\ldots,k_{q_s s}=-\infty}^{\infty} a_j \cdot \left[\prod_{p=1}^{q_1} J_{k_{p1}}\left(j\tilde{a}_{p1}^{\rm F}\right) \prod_{r=2}^{s}\prod_{p=1}^{q_r} J_{k_{pr}}\left(k_{p-1,r}\tilde{a}_{pr}^{\rm F}\right)\right] \cdot \sin\left[2\pi\left(jf_0 + \sum_{r=1}^{s}\sum_{p=1}^{q_r} k_{pr} p \tilde{f}_{\rm m}^r\right)t + \sum_{r=1}^{s}\sum_{p=1}^{q_r} k_{pr}\tilde{\varphi}_{pr}^{\rm F} + \tilde{\phi}_j\right]. \quad (42)$$

The frequency content is exactly the same as in the parallel case, only the values of amplitudes and phases are different.

3.3 The case of PM

Here we discuss the phase modulation. As we stated in the Sec. 2 there is no chance to distinguish between FM and PM phenomena on the basis of their measured signals (inverse problem), if the modulation function $m_{\rm m}^*(t)$ in Eq. (31) is allowed to be arbitrary. At the same time, if the basic physical parameters such as effective temperature, radius and $\log g$ are changing during the Blazhko cycle as was found recently (Sódor, Jurcsik & Szeidl 2009; Jurcsik et al. 2009a,b) the cyclic variation of the fundamental pulsation period (vis. frequency) that results in FM would be a plausible explanation for observed effects. There is an additional possible argument against the existence of PM in RR Lyrae stars.

If we assume that the modulating function $m_{\rm m}^*$ contains no explicit time variation – as in the usual definition for PM modulation in electronics – Eq. (31) reads as

$$m_{\rm PM}^*(t) = a_0 + \sum_{j=1}^{n} a_j \sin\left[2\pi j f_0 t + m_{\rm m}^*(t) + \varphi_j\right]. \quad (43)$$

When this formula is expressed as Eq. (33) or Eq. (35) according to a sinusoidal or an arbitrary periodic modulating function, respectively, the arguments of Bessel functions are independent from the harmonic order j as opposed to the case of FM. It causes a systematic difference between Fourier spectra of FM and PM. While the number of detectable side peaks in FM increases with the order of harmonics, for PM the number of side peaks is the same for all harmonics.

There are two Blazhko RR Lyrae stars that show both strong phase variations and their data are precise enough, these are the *CoRoT* targets V1127 Aql and CoRoT 105288363 (Chadid et al. 2010; Guggenberger et al. 2011). The spectrum of V1127 Aql clearly shows the existence of FM: 3rd order side frequencies are detected around the main pulsation frequency while order of 8th around the 19th harmonic. The Fourier analysis of separate Blazhko cycles of CoRoT 105288363 showed that with the increasing strength of phase variation, the number of detected side peaks around higher order harmonics are also increased (Guggenberger et al. 2011). It is an evidence of (changing) FM.

3.4 Real Blazhko stars with simultaneous AM and FM

In this section we discuss the general combined case, when both types of modulations occur simultaneously. As it was mentioned before both AM and FM type modulations were detected for all observed Blazhko RR Lyrae stars if the observed data sets were precise and long enough. This is the situation for ground-based (Jurcsik et al. 2009c; and references therein) and space-born observations of *CoRoT* and *Kepler* (Chadid et al. 2010; Poretti et al. 2010; Benkő et al. 2010; Kolenberg et al. 2011) as well.

Generalising the sinusoidal case of combined modulation Eq. (14) discussed in Sec. 2.3 we get

$$m_{\rm Comb}^*(t) = \left[1 + m_{\rm m}^*(t)\right] m_{\rm FM}^*(t), \quad (44)$$

where $m_{\rm FM}^*(t)$ is the general modulated FM function defined by Eq. (31). Since all observed Blazhko stars show AM and FM with the same frequency, we have investigated only those cases where this assumption is fulfilled.

3.4.1 Combined modulations with sinusoidal functions

The simplest case similarly to the pure AM and FM cases is the simultaneous but sinusoidal modulations.

$$m_{\rm Comb}^*(t) = (1 + h\sin 2\pi f_{\rm m} t)\cdot \left\{a_0 + \sum_{j=1}^{n} a_j \sin\left[2\pi j f_0 t + j a^{\rm F}\sin\left(2\pi f_{\rm m} t + \phi_{\rm m}\right) + \varphi_j\right]\right\}, \quad (45)$$

where the notations are the same or directly analogous with the previously defined ones: $h = a_{\rm m}/U_{\rm FM}^*$ and $U_{\rm FM}^*$ is the amplitude of the second term (the FM modulated "carrier wave"). The relative phase between AM and FM signals is $\phi_{\rm m} = \varphi^{\rm F} - \varphi_{\rm m}$.

According to the schema of (16) expression (45) can be reformulated into

$$m_{\rm Comb}^*(t) = a_0 + a_0 h \sin 2\pi f_{\rm m} t + \sum_{j=1}^{n}\sum_{k=-\infty}^{\infty} a_j \left\{J_k(ja^{\rm F})\sin\left[2\pi\left(f_0 + kf_{\rm m}\right)t + k\phi_{\rm m} + \varphi_j\right] + \frac{h}{2}J_{k-1}(ja^{\rm F})\sin\left[2\pi\left(f_0 + kf_{\rm m}\right)t + (k-1)\phi_{\rm m} + \varphi_j^-\right] + \frac{h}{2}J_{k+1}(ja^{\rm F})\sin\left[2\pi\left(f_0 + kf_{\rm m}\right)t + (k+1)\phi_{\rm m} + \varphi_j^+\right]\right\}, \quad (46)$$

where $\varphi_j^{\pm} = \varphi_j \pm \pi/2$. Based on Eq. (45) the Fourier spectrum in Fig. 16 can be interpreted as a sum of the combined modulation with sinusoidal carrier wave (16) with an additional term describing the modulation frequency itself (insert in bottom panel). Each harmonic is surrounded by a multiplet structure of peaks just like the main frequency. The number of side peaks increases with the harmonic order j similarly for FM (Sec. 3.2.1).

The asymmetrical amplitudes of pairs of side frequencies belonging to a given harmonic can be characterised similarly to the sinusoidal carrier wave case (18) as

$$\Delta_{jl} = -4\frac{hl}{ja^{\rm F}} a_j^2 J_l^2(ja^{\rm F})\sin\phi_{\rm m}. \quad (47)$$

Here $\Delta_{jl} = A^2(jf_0 + lf_{\rm m}) - A^2(jf_0 - lf_{\rm m})$ is the power difference of the lth side peaks at the jth harmonics ($l = 1, 2, \ldots$). Similarly to the course book case discussed in Sec. 2.3 the asymmetry depends on the actual value of h and $a^{\rm F}$, (viz. the relative

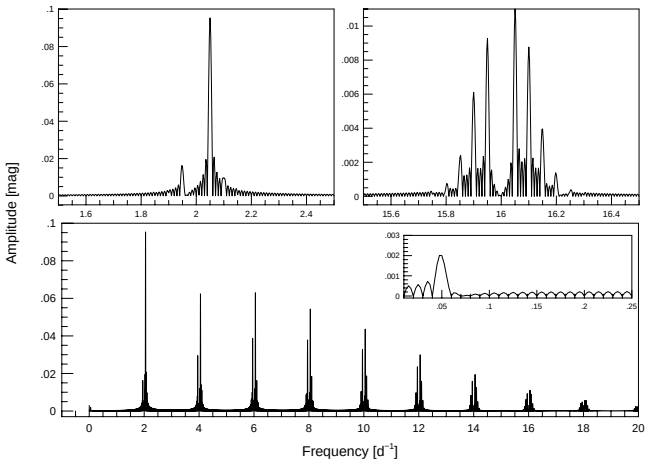

Figure 16. Bottom: Fourier amplitude spectrum of an artificial combined (AM & FM) light curve computed from Eq. (45) after the data are prewhitened with the main frequency and its harmonics. Top panels are zooms around the positions of the main frequency $f_0 = 2$ d^{-1} (top left), and its 7th harmonics $8f_0 = 16$ d^{-1} (top right), respectively. The relative phase between AM and FM is set to $\phi_{\rm m} = 270$ deg.

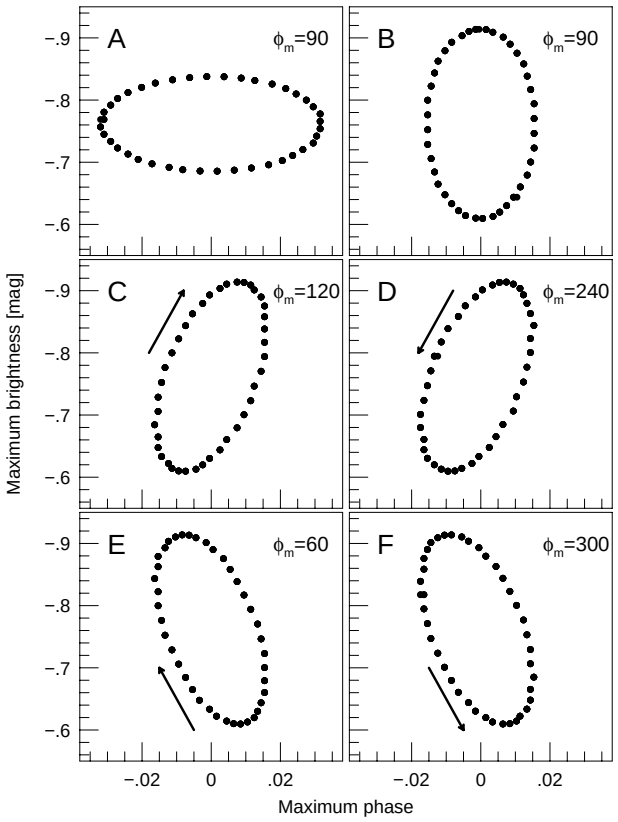

Figure 17. Maximum brightness vs. maximum phase diagrams for some artificial light curves with combined sinusoidal modulations. Between panels A and B the relative strengths of AM and FM are changed as (A) $h = 0.1$ and $a^{\rm F} = 0.2$ and (B) $h = 0.2$ and $a^{\rm F} = 0.1$, respectively. From panel B to F the amplitudes are fixed and only the relative phase $\phi_{\rm m}$ is changed as shown at the upper left corner in each panel. The arrows in panels C-F indicate the direction of motion.

strengths of AM and FM) and the relative initial phase angle $\phi_{\rm m}$. The most extreme possibility is when one of the side peaks completely disappears. The necessary conditions are $\phi_m = \pm\pi/2$ and $ja^{\rm F} = hl$. The asymmetry decreases with the increasing harmonic order j (see also top panels in Fig. 16), because all the Bessel functions quickly converge to zero with increasing arguments, therefore dominate the right hand side of expression (47).

Non-equidistant sampling and large gaps in the observed time series can cause significant differences between side-peak amplitudes (see Jurcsik et al. 2005). Such sampling effects, however, can not explain huge differences, such as when side peaks completely disappear in one side and the spectra show doublets, though numerous examples were found by large surveys as MACHO and OGLE (Alcock et al. 2000, 2003; Moskalik & Poretti 2003). But as illustrated by Fig. 16, highly asymmetrical side peaks can easily be generated by (45). This asymmetry effect can be a possible explanation for the observed doublets (RR-ν1 stars) and even for triplets (RR-ν2 stars). In the latter case the two side frequencies can originate from a quintuplet structure (equidistant triplet on one side) or from a multifrequency modulation (non-equidistant triplet on one side).

Searching for phases where the modulated and non-modulated light curves are identical we conclude that such phases exist only if $\phi_m = (k_1 - k_2)\pi$; (k_1, k_2 are integers) and then the moments of the coincidences are $t = k_2/2f_{\rm m}$. Assuming all Blazhko stars showing both AM and FM this conclusion supports the finding of Jurcsik, Benkő & Szeidl (2002), who studied light and radial velocity curves of Blazhko RR Lyrae stars,

The amplitude ratio vs. harmonic order diagrams show similar shapes and relative positions as were discussed in Sec. 3.2.2 with the connection of Fig. 13. Let us look at the maximum brightness vs. maximum phase diagrams, a classical tool for analysing Blazhko RR Lyrae stars. Such diagrams are plotted in Fig. 17 for synthetic light curves generated from the formula of (45). All diagrams have a simple round shape. They reflect the relative strength of AM and FM components. In panels A and B the relative strengths are opposite $2h = a^{\rm F}$ and $h = 2a^{\rm F}$, respectively. As a consequence, the loop is deformed vertically or horizontally. When the angle $\phi_{\rm m}$ differs from the special values of $l\pi/2$, ($l = 0, 1, 2, 3, 4$), the axes of the loops are inclined to the vertical horizontal position. This angle also determines the direction of motion. If $0 < \phi_{\rm m} < \pi$ it is clockwise, whilst if $\pi < \phi_{\rm m} < 2\pi$ it is anti-clockwise. (These conditions are the same as it was found by Szeidl & Jurcsik 2009 for sinusoidal carrier waves.) It is noteworthy, that the same ranges of $\phi_{\rm m}$ also determine the character of power difference of the side peaks: if the right hand side peaks are higher than the left hand side ones then the direction of motion is anti-clockwise and vice versa.

3.4.2 Non-sinusoidal combined modulation

On the basis of the previous sections it is easy to define the light curves which are modulated by general periodic signals simultaneously both in their amplitudes and phases:

$$m^*_{\rm Comb}(t) = \frac{m^*_{\rm AM}(t)}{c^*(t)} m^*_{\rm FM}(t), \qquad (48)$$

where the functions $m^*_{\rm AM}(t)$ and $m^*_{\rm FM}(t)$ are defined by Eqs. (23) and (34), respectively. Since the two modulations are described

by different functions (they are represented by different order of Fourier sums), no such simple relative phase can be defined as $\phi_{\rm m}$ for the sinusoidal case in Sec.3.4.1. Therefore, we obtain for the mathematical form of such a generally modulated light curve:

$$m^*_{\rm Comb}(t) = \left[a^{\rm A}_0 + \sum_{p'=1}^{q'} a^{\rm A}_{p'} \sin\left(2\pi p' f_{\rm m} t + \varphi^{\rm A}_{p'}\right)\right] \cdot \left\{a_0 + \sum_{j=1}^{n} a_j \sin\left[2\pi j f_0 t + j \sum_{p=1}^{q} a^{\rm F}_p \sin\left(2\pi p f_{\rm m} t + \varphi^{\rm F}_p\right) + \phi_j\right]\right\}, \quad (49)$$

where the notations are the same as in Eqs. (23) and (34). This expression describes all the discussed phenomena of a light curve modulated regularly with a single frequency $f_{\rm m}$. The envelopes of these light curves are very similar to the envelopes of non-sinusoidal AM light curves shown in Fig. 6. The light curves show non-sinusoidal phase variation as well (see also Figs. 10 and 14).

As in the former simpler cases, the Fourier spectrum can also be constructed analytically with the help of the sinusoidal decomposition of (49):

$$m^*_{\rm Comb}(t) = a_0 a^{\rm A}_0 + \sum_{p'=1}^{q'} a_0 a^{\rm A}_{p'} \sin\left(2\pi p' f_{\rm m} t + \varphi^{\rm A}_{p'}\right) + \sum_{j=1}^{n} \sum_{p'=0}^{q'} \sum_{k_1,k_2,\ldots,k_q=-\infty}^{\infty} \frac{a^{\rm A}_{p'}}{2} a_j \left[\prod_{p=1}^{q} J_{k_p}(j a^{\rm F}_p)\right] \cdot \sin\left\{2\pi\left[j f_0 + \left(\sum_{p=1}^{q} k_p p \pm p'\right) f_{\rm m}\right] t + \psi^{\pm}_{pp'j}\right\}. \quad (50)$$

Here the $\psi^{\pm}_{pp'j} := \sum_{p=1}^{q} k_p \varphi^{\rm F}_p \pm \varphi^{\rm A}_{p'} + \phi_j \mp \pi/2$, the arbitrary constant is chosen as $\varphi^{\rm A}_0 := \pi/2$. The qualitative structure of this spectrum is simple and well-understandable on the basis of the previously discussed cases. The second term is responsible for the appearance of the modulation frequency and its higher harmonics (see insert in Fig. 7). The next (infinite number of) terms describe a spectrum which is similar to the non-sinusoidal FM spectrum (Fig. 12) but it also shows the AM splitting which is present in the sinusoidal combined case. These effects make the calculation of the peaks' amplitude complicated. The asymmetry between each pair from a multiplet around a given harmonic is determined by two factors: one of them is the the non-sinusoidal nature of the FM (Sec. 3.2.2) and the other one is the combination of AM and FM (Sec. 3.4.1).

The maximum brightness vs. maximum phase diagrams generally show complicated shapes. They could form knots, loops and other non-trivial features. A collection of such diagrams is plotted in Fig. 18. The direction of the motion can arbitrarily change by tuning the initial phases.

3.4.3 Combined multifrequency modulations

A combined modulation with multiperiodic AM or FM or both can be handled analogously to the simpler presented cases. We can substitute $m^*_{\rm m}(t)$ into the general expression (44) as it was defined by Eq. (25) (parallel AM) or Eq. (28) (AM cascade). Writing $m^*_{\rm FM}(t)$ as Eq. (38) (parallel FM) or Eq. (40) (FM cascade) in principle is straightforward. In practice, however, calculating coefficients (amplitudes, phases) is more complicated. The resulting light curves and Fourier spectra can be interpreted on the basis of their constituents. They do not show new features except their maximum brightness vs. maximum phase diagrams which show time-dependent and generally non-closed curves as opposed to those in Fig 18. If the ratio of modulating frequencies are commensurable, the curve is closed, otherwise it has a non-repetitive behaviour. The reason is that if the modulation is described by N independent frequencies the proper diagram would be $2N$-dimensional and the classical one is only a 2-D projection of it.

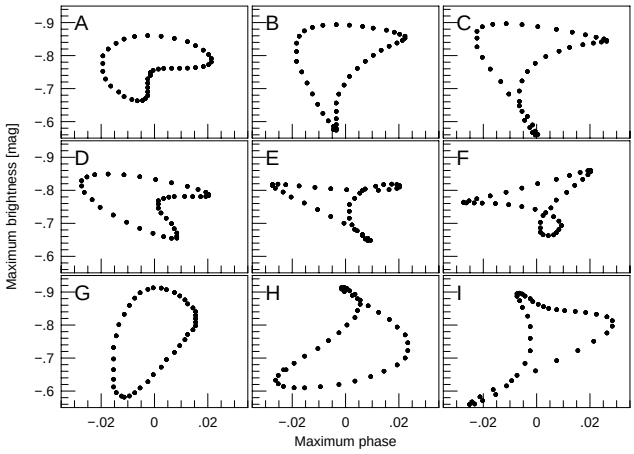

Figure 18. Some typical maximum brightness vs. maximum phase diagrams for synthetic light curves with combined non-sinusoidal modulations. The relative strength, initial phases and number of used harmonics of AM and FM has been varied.

4 PRACTICAL APPLICATION – A CASE STUDY

To demonstrate how our formalism works in practice, we generated two artificial light curves with simultaneous non-sinusoidal AM (with two harmonics, $p' = 2$) and FM (with three harmonics, $p = 3$). The light curves are 100-days long and sampled by 5-minutes in the same manner as the all synthetic light curves in the paper. We added Gaussian noise to the light curves either with rms=0.01 mag (model A) or 10^{-4} mag (model B), respectively. The model A is similar to a good quality ground-based observation, while the model B simulates a typical space-borne data set. These two artificial light curves (top panels in Fig. 19) were analysed with a blind test (i.e. without knowledge about frequencies, amplitudes and phases) both by the traditional way and by our method.

4.1 Classical light curve analysis

Constructing the mathematical model Eq. (19) of the light curves in the traditional analysis is a successive prewhitening process. It consists of Fourier spectra building, fitting the data with the parameters of the highest peak(s) in the spectrum by a non-linear algorithm, and subtracting the fitted function from the data and so on. The process continues as long as significant peaks are detected. At the end of this analysis the noise of the residual data reaches the observational scatter.

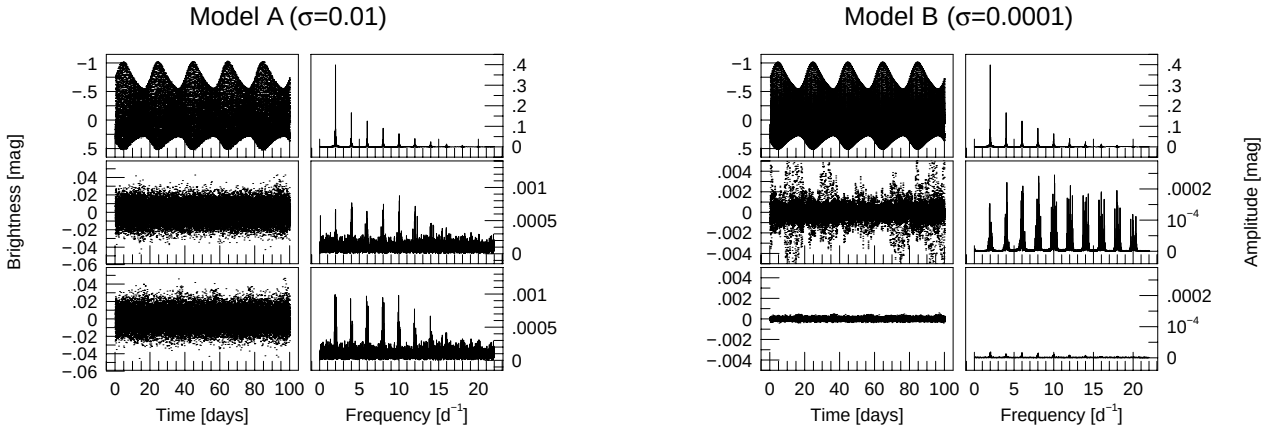

Figure 19. Artificial light curves with Gaussian noise and their Fourier spectra. Model A ($\sigma = 10^{-2}$) is plotted in the left, model B ($\sigma = 10^{-4}$) in the right. The residual light curves and their spectra after the traditional fitting process (middle panels) and the present one (bottom panels). (Residuals and their spectra are in different scales for the two models.)

In the case of model A the highest peaks belong to the main frequency f_0 and its harmonics. In the further prewhitening steps the triplets ($f_0 \pm f_\mathrm{m}$), quintuplets ($f_0 \pm 2f_\mathrm{m}$), septuplets ($f_0 \pm 3f_\mathrm{m}$), nonuplets ($f_0 \pm 4f_\mathrm{m}$) and the modulation frequency (f_m) were found and fitted. The significance level was chosen at $S/N = 4$, where signal-to-noise ratio (S/N) is estimated as Breger et al. (1993). To remove all significant peaks from the spectrum five from the undecaplet peaks ($f_0 + 5f_\mathrm{m}$) and two aliases have to be fitted and subtracted. (We note that the frequency $2f_\mathrm{m}$ was detectable, but under the significance level, therefore it was not fitted.) The residual light curve of this process and its Fourier spectrum are plotted in the middle panels of Fig. 19. The rms of the residual light curve is 10^{-2}, so we got back the input noise value. The number of fitted frequencies are 103 and used parameters in this successive fit is 201. If the frequency of the side peaks are also fitted independently ("let it free approach") this value increases to 286.

The process works similarly in the case of model B as well. Naturally, many more significant peaks are detectable. From the highest peaks to the lowest: f_0, its harmonics, the side peaks up their orders of six ($f_0 \pm 6f_\mathrm{m}$), the modulation frequency and its harmonic (f_m, $2f_\mathrm{m}$) are significant. Many alias peaks originating from the finite data length are also detectable: 46 such frequencies were removed up to the significance level of the sixth order of side peaks. We stopped the analysis here at $S/N \approx 40$, because we already found 168 frequencies and used 368 parameters (or 478 if we fit each frequency independently). The resulted light curve and its Fourier spectrum are shown in the middle panels of Fig. 19. The rms of this light curve is 10^{-3} an order of magnitude higher than the input noise parameter is.

4.2 Light curve analysis in our framework

When we apply the approach of this work we need to calculate only one Fourier spectrum and a single non-linear fit for each light curve. The Fourier spectrum and the characteristics of the light curve help us to choose the proper fitting formula and to determine the initial values of the fit.

The Fourier spectrum for any of the light curves A and B provide us with the necessary parameters (f_0, j, a_0, a_j, φ_j) of the carrier wave. The amplitude modulation and its non-sinusoidal nature in both light curves are apparent. Searching for peaks in the low frequency range of the Fourier spectra results in good initial values for f_m, $p' = 1, 2$, $a_{p'}^\mathrm{A}$ and $\varphi_{p'}^\mathrm{A}$. While more side peaks are detectable around the harmonics of the main frequency than the number of harmonics of f_m and the side peaks are asymmetrical, an FM has to be assumed. To check its non-sinusoidal nature we may prepare e.g. an O−C or maximum brightness vs. maximum phase diagram. At the end of this preparatory work we can choose the fitting formula (49). We note that to determine the correct initial values of a_p^F and φ_p^F depends on the tool used for finding the frequency variations. In the worst case, they can be estimated by some numerical trials with the non-linear fit. Using initial values that are good enough the non-linear fit converged fast for models A and B. The algorithm reached the noise levels 10^{-2} and 10^{-4} within few (less than 10) iterations automatically. The residual light curves and their Fourier spectra are plotted in the bottom panels of Fig 19. The number of fitted parameters for both models is only 33. Due to the finite numerical accuracy the residual spectra always show a structure reflecting the original spectra at very low levels.

In conclusion our method fits the light curves in a single step with much less parameters than the traditional one. In addition we avoid the time-consuming alias fitting and subtracting processes. The difference in the number of used parameters increases with the increasing accuracy of the observed data sets. In our example the number of regressed parameters is reduced from 6 times (model A) to more than 10 times (model B). Our description has advantages in the numerical fit of the ground-based observations as well, but its advantages are outstanding in the analysis of the space-born time series.

5 DISCUSSION AND SUMMARY

In this paper we have investigated mathematical representation of artificial light curves. These light curves are defined as modulated signals where their carrier wave is a monoperiodic RR Lyrae light curve defined by its finite Fourier sum. Different types of periodic functions are taken into account as modulation functions from the

Table 1. A schematic table for classifying different types of single frequency modulations from their light curves and Fourier spectra. The indices l and k are integers, where l is a finite number, while k can generally be infinite.

modulation	phenomenon	AM	FM	Combined
sinusoidal	amplitude variations:	yes (simple)	no	yes (simple)
	phase variations:	no	sinusoidal	sinusoidal
	side peak structure:	triplets ($jf_0 \pm f_\mathrm{m}$)	multiplets ($jf_0 \pm kf_\mathrm{m}$)	multiplets ($jf_0 \pm kf_\mathrm{m}$)
	side peak amplitudes:	symmetrical	symmetrical	asymmetrical
	modulation frequency:	f_m	–	f_m
non-sinusoidal	amplitude variations:	yes (complex)	no	yes (complex)
	phase variations:	no	non-sinusoidal	non-sinusoidal
	side peak structure:	multiplets ($jf_0 \pm lf_\mathrm{m}$)	multiplets ($jf_0 \pm kf_\mathrm{m}$)	multiplets ($jf_0 \pm kf_\mathrm{m}$)
	side peak amplitude:	symmetrical	asymmetrical	asymmetrical
	modulation frequencies:	lf_m	–	lf_m

simple sinusoidal to multiperiodic and general ones. The consequences of these modulation functions and modulation types (AM, FM, combined) are reviewed and presented.

We followed a step-by-step analysis from the simplest case to the more complicated ones. The results of this process can be summarized as follows:

- (i) Tuning AM by the used modulation function, namely the number of harmonic terms and their amplitudes and phases, the *synthetic light curves* reproduce well the observed shape of the Blazhko envelope curves. This is always true for the envelopes of maxima, however, the envelope of minima are affected by the fine structure of the bump and its phase shift along the light curve and changing shapes. These variations in the shock are associated to the Blazhko modulation such a way that a displacement of the shock forming region occurs over the Blazhko cycle. This induces an earlier or later occurrence of the bump in the light curves (see Preston et al. 1965). If these variations are strong enough, the envelope curve of minima could be different from our simple modulated ones. (ii) We showed that AM with extremely high modulation depth ($h > 1$) might be an explanation for the strange light curve shape of V445 Lyrae observed by *Kepler*. (iii) When the AM function depends on more than one frequency, (in a parallel or cascade modulation) we can generate envelope curves with different observed phenomena such as beating effect, alternating maxima, long-term, periodic amplitude changes.
- *Fourier spectra of AM cases* can be easily classified (see also Table 1). For a periodic modulation the signal represented by a finite Fourier sum the spectrum of the synthetic light curve shows the modulation frequency, multiplets around the pulsation frequency and its harmonics, as well. The order of multiplets (the number of peaks on one side) is the same as the used number of terms for describing the modulation function. As a special case, the sinusoidal modulation results in triplet structures and the appearance of f_m only. For a multiperiodic parallel modulation, the spectrum consists of a sum of the frequencies of each component modulation, while in the case of modulated modulation (AM cascade) spectra includes additional peaks at the all possible linear combination frequencies, as well.
- For all AM cases the Fourier *amplitude of the side frequencies* are proportional to the given harmonics' amplitude, therefore, the numbers and the side peak amplitude ratios compared to the central frequencies are the same for all orders of harmonics. Pure AM results in symmetrical multiplets: side frequencies of the same order have the same amplitudes.
- The *variation of the mean brightness* through the Blazhko cycle is a consequence of the AM modulation. The effect appears even for the simplest sinusoidal modulation function, and is closely related to the appearance of the modulation frequency itself in the Fourier spectrum.
- Pure *FM light curves* have no amplitude changes but significant phase variations. Their Fourier spectra show multiplet structure around the pulsation frequency and its harmonics even for the simplest sinusoidal modulation. As opposed to AM the detectable number of side peaks is increasing with the increasing harmonic orders. The modulation frequencies (and their harmonics) are absent in the spectra. The side peaks' structure can be symmetrical (for sinusoidal modulation) or asymmetrical (most of the non-sinusoidal cases). The non-sinusoidal FM can be characterized by the classical O−C tool. The multifrequency FM spectra include all possible linear combination frequencies in the parallel case.
- The *Fourier amplitude ratio of the side peaks vs. harmonic orders* are determined by the Bessel functions of the first kind (for the sinusoidal case) or their product (for the non-sinusoidal case). As a consequence, these relationships are generally non-strictly decreasing with the increasing harmonic orders. Therefore, we can find larger amplitudes for the higher-order side peaks than for the lower-orders ones for comparing the same order of side peaks around different harmonics and different order of side peaks around a given harmonic. The latter can be true also for the amplitude of the side peaks and the central peaks' (the harmonics') amplitude.
- The simultaneous AM and FM show all the above mentioned effects. The side peaks' amplitudes in the Fourier spectra of the combined modulations are generally asymmetrical already for sinusoidal AM and FM. The asymmetry can totally remove side peak(s) in one side. The strength of asymmetry depends on the initial phase difference of the AM and FM modulation functions. This phase difference determines both the inclination and direction of motion of the loop in the maximum brightness vs. maximum phase diagram.
- In the case of the pure sinusoidal AM and FM (and with very special parameters for non-sinusoidal and combined cases as well), there are well-defined phases where the modulated and non-modulated light curves are identical. However, we have pointed out that, when a star shows general combined modulation (even a sinusoidal one), its light curve is always different from any monoperiodic (non-modulated) stars.
- We showed that our modulation description presented here needs much (typically 3–10 times) less parameters for fitting a light curve than the classical solution, where all detected frequencies have their own independent amplitude and phase. The prize to pay for the relatively small number of parameters is the more compli-

cated fitting formulae. Our approach fits the light curves only once, instead of the traditional successive prewhitening process, and unaffected by most aliasing problems.

It is equally important to list those observed features that do not follow this picture. One of these effects is the *phase lag*, a difference between the Blazhko phases of maxima of maxima and minima of minima of the modulated light curves. These phase lags can be several pulsation cycles long. In our study, however, all envelopes are highly symmetrical: their maxima and minima are practically at the same Blazhko phases. If we see the well-sampled observed light curves (e.g. *CoRoT* or *Kepler* data) showing this phase lag, we can realise that the effect builds up from the systematic motions and changing the shape of the bump caused by the hydrodynamical shock in the RR Lyrae atmospheres.

An additional unsolved problem is the *distribution of the side peaks' asymmetry*. The large surveys (OGLE, MACHO) found that the spectra of Blazhko RR Lyrae stars more frequently contain asymmetrical side frequency patterns, where the higher frequency side peaks have the higher amplitude than vice versa (e.g. 74 vs. 26 per-cents for LMC by Alcock et al. 2000). All formulae suggest 50-50 per-cents of probabilities, if the distribution of the relative phases between AM and FM is uniform. The detected asymmetrical distribution might have deeper physical origin.

Our description does not explain the *additional frequencies* such as half-integer frequencies belonging to period doubling, temporary overtone frequencies and further exotic frequencies in the Fourier spectra, recently discovered from the space data (Gruberbauer et al. 2007; Kolenberg et al. 2010; Szabó et al. 2010; Chadid et al. 2010; Poretti et al. 2010; Benkő et al. 2010). Their connection with the physics of Blazhko effect is poorly understood and their modelling is out of the scope of this paper.

The main result of this analysis is the demonstration that the modulation paradigm gives successfully accounts for most of the observed properties of Blazhko RR Lyrae light curves. Moreover, this work may help to distinguish between those features that have deeper physical origin from those ones which appear simply due to the modulation. This framework seems to be very flexible and can easily be generalised to a larger fraction of variable stars taking into account, e.g., multifrequency carrier waves or stochastic modulations.

ACKNOWLEDGMENTS

This project has been partially supported by the ESA PECS projects No. 98022 & 98114, and the Hungarian OTKA grant K83790. R.Sz. thanks the support of the János Bolyai Research Scholarship of the HAS. The authors thank to the referee Dr. Katrien Kolenberg for her helpful comments and close reading of the manuscript.

REFERENCES

Abramowitz M., Stegun I. A., 1972, Handbook of Mathematical Functions, 10th issue, National Bureau of Standards, Washington D.C.
Alcock C. et al., 2000, ApJ, 542, 257
Alcock C. et al., 2003, ApJ, 598, 597
Benkő J. M. et al., 2009, AIP Conf. Proc. 1170, 273
Benkő J. M. et al., 2010, MNRAS, 409, 1585
Blazhko S. N., 1907, Astron. Nachr., 175, 325
Breger M. 2010, in Sterken C., Samus' N. N., Szabados L., eds, Variable Stars, the Galactic halo and Galaxy Formation, Sternberg Astronomical Institute, Moscow, p. 95
Breger M., Kolenberg K., 2006, A&A, 460, 167
Breger M. et al., 1993, A&A, 271, 482
Carson J. R., 1922, Proc. IRE, 10, 57
Cartianu Gh., 1966, Frequency Modulation, Academic Press, Bucharest
Chadid M. et al., 2009, in Guzik J. A., Bradley P., eds, AIP Conf. Proc. 1170, Stellar Pulsation: Challanges for Theory and Observation, p. 235
Chadid M. et al., 2010, A&A, 510, A39
Chowning J. M., 1973, J. Audio Eng. Soc., 21, 526
Derekas A., Kiss L. L., Udalski A., Bedding T. R., Szatmáry K., 2004, MNRAS, 354, 821
Gruberbauer M. et al., 2007, MNRAS, 379, 1498
Guggenberger E., Kolenberg K., Chapellier E., Poretti E., Szabó R., Benkő J. M., Paparó M., 2011, MNRAS, accepted (astro-ph/1104.1726)
Henry G. W., Fekel F. C., Henry, S. M., 2005, AJ, 129, 2815
Hurta Zs., Jurcsik J., Szeidl B., Sódor Á., 2008, AJ, 135, 957
Jurcsik J., Benkő J. M., Szeidl B., 2002, A&A, 390, 133
Jurcsik J. et al., 2005, A&A, 430, 1049
Jurcsik J. et al., 2008, MNRAS, 391, 164
Jurcsik J. et al., 2009a, MNRAS, 393, 1553
Jurcsik J. et al., 2009b, MNRAS, 397, 350
Jurcsik J. et al., 2009c, MNRAS, 400, 1006
Koen C., 2001, MNRAS, 322, 97
Kolenberg K. et al., 2006, A&A, 459, 577
Kolenberg K. et al., 2010, ApJ, 713, L198
Kolenberg K. et al., 2011, MNRAS, 411, 878
Kovács G., 1995, A&A, 295, 693
Kurtz D. W. et al., 2000, in Szabados L., Kurtz D. W., eds, The Impact of Large-Scale Surveys on Pulsating Star Research, ASP Conf. Ser. 203, p. 291
LaCluyzé A. et al., 2004, AJ, 127, 1653
Moskalik P., Poretti E., 2003, A&A, 398, 213
Moskalik P., Kołaczkowski Z., 2009, in Goupil M., Kolláth Z., Nardetto N., Kervella P., eds, Nonlinear Pulsations and Hydrodynamics of Cepheids, EAS Publ. Ser. 38, p. 83
Nagy A., 1998, A&A, 339, 440
Newkirk D., Karlquist R., 2004, in The ARRL Handbook for Radio Communications (81st ed.), Reed D. G., ed., pp. 15.1-15.36, Newington
Poretti E. et al., 2010, A&A, 520, A108
Poretti E. et al., 2011, A&A, 528, A147
Preston G. W., Smak J., Paczyński B., 1965, ApJSS, 12, 99
Roder H., 1931, Proc. IRE, 19, 2145
Schottstaedt W., 1977, Computer Music J., 1, 46
Schottstaedt W., 2003, An Introduction to FM, https://ccrma.stanford.edu/software/snd/snd/fm.html
Sódor Á. et al., 2006, IBVS, 5705
Sódor Á., Jurcsik J., Szeidl B., 2009, MNRAS, 394, 261
Sódor Á. et al., 2011, MNRAS, 411, 1585
Sterken C., 2005, in Sterken C., ed., The Light-Time Effect in Astrophysics, ASP Conf. Ser. 335, p. 3
Stothers R. B., 2010, PASP, 122, 536
Szabó R. et al., 2010, MNRAS, 409, 1244
Szczygieł D. M., Fabrycky D. C., 2007, MNRAS, 377, 1263
Szeidl B., Jurcsik J., 2009, CoAst, 160, 17
van der Pol B., 1930, Proc. IRE, 18, 1194
Wils P., Kleidis S., Broens E., 2008, MNRAS, 387, 783

APPENDIX A: ABOUT THE EXACT FOURIER TRANSFORMS

There are many definitions of the Fourier transform, differing from each other by their normalizations. In this paper we adhere to the following definition:

$$\mathcal{F}(f) = \int_{-\infty}^{\infty} g(t) \mathrm{e}^{-\mathrm{i}2\pi f t} dt. \quad \text{(A1)}$$

Since we always transform our equations describing the different types of modulated signals to linear combinations of sinusoidal functions, it is necessary to know the exact Fourier transformation of these elements.

The Fourier transform of the sinusoidal carrier wave Eq. (1) itself is

$$\mathcal{F}\left[c(t)\right] = \pi\sqrt{2\pi}U_{\mathrm{c}} \left\{\mathrm{i}\cos\varphi_{\mathrm{c}}\left[\delta(f-f_{\mathrm{c}}) - \delta(f+f_{\mathrm{c}})\right] + \sin\varphi_{\mathrm{c}}\left[\delta(f-f_{\mathrm{c}}) + \delta(f+f_{\mathrm{c}})\right]\right\}, \quad \text{(A2)}$$

where i is the imaginary unit, δ is the Dirac function. As we see, the Fourier amplitude spectrum belonging to $c(t)$ has two components: one at positive frequency (centred on $+f_{\mathrm{c}}$) and one at negative frequency (centred on $-f_{\mathrm{c}}$). We concern only the positive frequency, since the negative ones have no physical meaning.

Demonstrating the use of the above formulae, the positive part of the Fourier transformation of the sinusoidal AM signal (4) is given:

$$\mathcal{F}^{+}\left[U_{\mathrm{AM}}(t)\right] = \mathcal{F}^{+}\left[c(t)\right] + \pi\sqrt{\frac{\pi}{2}}U_{\mathrm{m}}\left[\left[\cos(\varphi_{\mathrm{c}}-\varphi_{\mathrm{m}}) + \mathrm{i}\sin(\varphi_{\mathrm{c}}-\varphi_{\mathrm{m}})\right]\delta(f+f_{\mathrm{c}}-f_{\mathrm{m}}) - \left[\cos(\varphi_{\mathrm{c}}+\varphi_{\mathrm{m}}) + \mathrm{i}\sin(\varphi_{\mathrm{c}}+\varphi_{\mathrm{m}})\right]\delta(f+f_{\mathrm{c}}+f_{\mathrm{m}})\right]. \quad \text{(A3)}$$

According to this schema, the investigated signals describing the more complicated expressions can also be calculated in a straightforward way.

APPENDIX B: GENERALIZED PRODUCT-TO-SUM FORMULAE

Let us calculate the generalised form of the product-to-sum expression from the well-known identity of trigonometry:

$$\sin(\alpha_1)\sin(\alpha_2) = \frac{1}{2}[\cos(\alpha_1-\alpha_2) - \cos(\alpha_1+\alpha_2)]. \quad \text{(B1)}$$

Assuming n factor in the left-hand-side it can be formally written as $\prod_{i=1}^{n}\sin\alpha_i$. Introducing the vector-scalar function $\mathcal{S}_n(\boldsymbol{\alpha}) := \prod_{i=1}^{n}\sin\alpha_i$, $\boldsymbol{\alpha} = (\alpha_1, \alpha_2, \ldots, \alpha_n)^{\mathrm{T}}$, where T indicates transposition, and applying the formula (B1) n times recursively we arrive to

$$\mathcal{S}_n(\boldsymbol{\alpha}) := \begin{cases} 2^{(1-n)} \sum_{l=1}^{2^{(n-1)}} (-1)^N \cos\left(\sum_{i=1}^{n} Q_{li}\alpha_i\right) & \text{if } n \text{ even}, \\ 2^{(1-n)} \sum_{l=1}^{2^{(n-1)}} (-1)^{N'} \sin\left(\sum_{i=1}^{n} Q_{li}\alpha_i\right) & \text{if } n \text{ odd}, \end{cases} \quad \text{(B2)}$$

where

$$N = \frac{3n}{2} - \sum_{i=1}^{n} Q_{li}, \quad \text{and} \quad N' = \frac{3(n-1)}{2} - \sum_{i=1}^{n} Q_{li}.$$

Each sin/cos term includes a sum of n terms of the α_i angles inside their arguments as $\alpha_1 \pm \alpha_2 \pm \alpha_3, \cdots \pm \alpha_n$. One combination from these sets contains l positive and $n-l$ negative angles. The total number of such a combination is 2^{n-1}. Each row of the matrix Q contains the signs of the angles of a possible set from the total number of 2^{n-1}. Namely, the elements of the matrix Q are either $+1$ or -1, but $Q_{l1} = 1$ i.e. the first columns contain $+1$ for all ls.

This paper has been typeset from a TEX/ LATEX file prepared by the author.